Inhibition of the ULK1 protein complex suppresses *Staphylococcus*-induced autophagy and cell death

Ohood A. Radhi[1#]**, Scott Davidson**[1]**, Fiona Scott**[2]**, Run X. Zeng**[3]**, D. Heulyn Jones**[2]**, Nicholas C.O. Tomkinson**[2]**, Jun Yu**[1]**, Edmond Y.W. Chan**[1,3,4*]

From: [1] Strathclyde Institute for Pharmacy and Biomedical Science, University of Strathclyde, United Kingdom; [2] WestCHEM, Department of Pure and Applied Chemistry, University of Strathclyde, United Kingdom; [3] Department of Biomedical and Medical Sciences, [4] Department of Pathology and Molecular Medicine, Queen's University, Canada.

Running title: *ULK1 inhibition suppresses Staphylococcus infection*

[#] Present address: Department of Basic science, College of Nursing, University of Kufa, Iraq

[*] Corresponding author: Tel +1-613-533-6946, E-mail: eywc@queensu.ca

_____

Abstract

Autophagy plays multiple roles in host cells challenged with extracellular pathogens. Here, we aimed to explore whether autophagy inhibition could prevent bacterial infections. We first confirmed widely distinct patterns of autophagy responses in host cells infected with *Staphylococcus* aureus, as compared with *Salmonella*. Only infection with *Staphylococcus* produced strong accumulation of lipidated autophagy-related protein LC3B (LC3B-II). Infection with virulent *Staphylococcus* strains induced formation of p62-positive aggregates, suggestive of accumulated ubiquitinated targets. During *Salmonella* infection, bacteria remain enclosed by lysosomal-associated membrane protein 2 (LAMP2)-positive lysosomes, whereas virulent *Staphylococcus* apparently exited from enlarged lysosomes and invaded the cytoplasm. Surprisingly, *Staphylococcus* appeared to escape from the lysosome without generation of membrane-damage signals as detected by Galectin3 recruitment. In contrast, *Salmonella* infection produced high levels of lysosomal damage, consistent with a downstream antibacterial xenophagy response. Lastly, we studied the Unc-51-like autophagy-activating kinase 1 (ULK1) regulatory complex, including the essential subunit autophagy-related protein 13 (ATG13). Infection of cells with either *Staphylococcus* or *Salmonella* led to recruitment of ATG13 to sites of cytosolic bacterial cells to promote autophagosome formation. Of note, genetic targeting of ATG13 suppressed autophagy and the ability of *Staphylococcus* to infect and kill host cells. Two different ULK1 inhibitors also prevented *Staphylococcus* intracellular replication and host cell death. Interestingly, inhibition of the ULK1 pathway had the opposite effect on *Salmonella*, sensitizing cells to the infection. Our results suggest that ULK1 inhibitors may offer a potential strategy to impede cellular infection by *Staphylococcus* aureus.

_____

Macro-autophagy (often referred to simply as autophagy) is an intracellular degradation pathway that functions as a starvation-dependent metabolic response but also as a critical housekeeping mechanism to eliminate damaged organelles (1). A third important set of pathways relates to roles of autophagy for host cell-pathogen interactions during bacterial infection. In this way, autophagy has been shown to degrade and restrict the replication of certain types of invading bacteria, leading to the initial definition of the dedicated pathway, xenophagy (foreign-eating) (2-6).

The xenophagy response following *Salmonella* infection has particularly been well investigated. Following invasion of host cells, gram-negative *Salmonella enterica* promote membrane remodelling that enables the bacteria to reside

1

within specialized *Salmonella*-containing vacuoles (SCV). Bacteria can then take one of several fates depending on cell context and environmental factors. Due to SCV damage, some bacteria escape to the cytoplasm and are recognised by ubiquitination systems regulated by host E3 ligases such as leucine-rich repeat and sterile α motif-containing 1 (LRSAM1) (7), linear ubiquitin chain assembly complex (LUBAC) and Ariadne RBR E3 Ubiquitin Protein Ligase 1 (ARIH1) (8,9). The concerted action of these pathways produce mixed linear and branched ubiquitin chains (10-12) that serve as primary eat-me signals to recruit ubiquitin-binding adaptor proteins (13,14). A number of xenophagy adaptor proteins have been identified including the proto-typical family member p62/sequestosome 1 (SQSTM1) (15) which functions during *Salmonella* infection together with other adaptors such as nuclear dot protein 52 kDa (NDP52, also called CALCOCO2) (16-18) and optineurin (15,18-20). An additional atypical adaptor protein, Tax1-binding protein 1 (TAX1BP1), further support xenophagy of *Salmonella* (21). Together, these adaptors form complexes that bridge ubiquitin-coated bacteria to Autophagy-related protein 8 (ATG8) family members such as LC3 on autophagy elongation membranes (15,22,23). In this way, cytosolic *Salmonella* are captured into autophagosomes for transport to lysosomal compartments, where they are effectively neutralized.

In contrast to xenophagy, other types of bacteria, including Gram-positive *Staphylococcus aureus*, have evolved to subvert and exploit the autophagy pathway to support their replicative life cycle. Methicillin-resistant *Staphylococcus aureus* (MRSA) now encompasses a wide collection of strains that have evolved over the last 60 years to become broadly insensitive to beta-lactam antibiotics including penicillin and amoxicillin (24). MRSA is still one of the leading causes of nosocomial infections with a wide range of targets from skin wounds to internal soft tissues. While *Staphylococcus aureus* was initially considered an extracellular pathogen, it is now appreciated that these bacteria can survive after internalization into professional phagocytes (e.g. macrophages and neutrophils) and non-professional (non-phagocytic) cells (e.g.

osteoclasts and fibroblasts) (25). *In vivo*, the fraction of *Staphylococcus aureus* that persists intracellularly gains protection from further antibiotics to eventually escape and spread bacteria beyond the initial site of infection (26). As such, the intracellular pool of *Staphylococcus aureus* could be a significant underlying contributor towards chronic or recurrent infection.

While anti-bacterial xenophagy during *Salmonella* infection has been extensively characterized, there are relatively fewer studies on *Staphylococcus aureus* and roles of autophagy. During *Staphylococcus* infection, bacteria internalize via phagocytosis to enter an endosomal compartment that is initially Rab5- and subsequently Rab7-positive (27,28). Although still controversial, evidence indicates that *Staphylococcus* utilize a number of virulence systems to prevent full activation of the phagolysosomal degradative compartment to enable survival (25). Virulent strains of *Staphylococcus aureus* express multiple factors including alpha-haemolysin and phenol soluble modulins which mediate endosome remodelling, membrane disruption and eventual bacterial escape into the cytoplasm, particularly in non-phagocytic cell types (29-31). At this stage, free cytosolic *Staphylococcus aureus* or bacteria within damaged phagosomes are captured by autophagosomal membranes. Once within autophagosomes, *Staphylococcus* virulence factors are proposed to further inhibit fusion with lysosomes or acidification of the autolysosome to generate a permissive membrane-enclosed niche for bacterial replication (28,32). The importance for this autophagy-dependent niche was highlighted by evidence of inhibited *Staphylococcus aureus* infection in mouse embryonic fibroblasts lacking autophagy protein ATG5 (28). However, the role of autophagy during *Staphylococcus aureus* infection across different host cell and strain contexts is not well understood. One report has suggested that autophagosomes transport *Staphylococcus* to acidic lysosomal compartments for degradation (33). Other evidence has suggested that *Staphylococcus* replication does not require autophagy and targeting of bacteria via an ubiquitin-dependent xenophagy pathway (34).

2

Here, we investigated details of the autophagy-*Staphylococcus aureus* interaction since better understanding in this area could have potential medical applications. Using non-phagocytic cell hosts, we found that MRSA infection led to strong markers of autophagy activation. *Staphylococcus* could be detected replicating inside lysosomal-like niche compartments but with minimal levels of membrane damage. MRSA infection led also to strong accumulation of ubiquitin-associated aggregates but these did not localise directly around bacteria. In parallel investigation, we found that *Salmonella* infection generated distinct patterns of remodelling in the host cell autophagy-lysosomal pathway. Moreover, we found that the ability of MRSA to infect and kill non-phagocytic cells was highly dependent upon autophagy. Inhibition of the canonical autophagy ULK1 regulatory kinase complex was sufficient to completely block infection and restore viability to host cells. Our results therefore identify an autophagy kinase pathway that can be targeted by small molecules to suppress cellular infection by MRSA.

Results

Activation of autophagy following infection by *Staphylococcus aureus*

We aimed to first study how different bacterial pathogens activate the autophagy pathway. For this test, autophagy was monitored by western blotting for the prototypical ATG8 family member, LC3B. Normally, LC3 is synthesised and cleaved during autophagy to generate mature LC3-I which is lipidated during autophagy activation to generate the LC3-II form which associates with autophagosomes (35). In initial experiments, we compared *Staphylococcus aureus* (ATCC29213) and *Salmonella enterica sv. Typhimurium* (NCTC13347), as common reference strains used for xenophagy studies (2,28). HeLa cells were infected with *Staphylococcus aureus* following a previously described protocol (28). To allow direct comparison, cells were infected with *Salmonella enterica sv. Typhimurium* by the same method. Briefly, both pathogens were grown until OD=0.3 and added to infect cells at MOI 200 for three

hours (Figure 1A). To compare xenophagy responses with standard autophagy, parallel cell samples were treated as controls to either amino acid starvation or the autophagy/lysosome inhibitor chloroquine. Interestingly, strongest levels of LC3B-II accumulation and highest LC3B lipidation ratios were detected when cells were infected with ATCC29213. Incubation of HeLa cells with chloroquine to block the autophagy/lysosomal pathway also led to accumulation of LC3B-II formed under basal levels of autophagy activation. In contrast, during a typical starvation response, LC3 is activated to form LC3-II, which is then quickly degraded via the lysosome reflecting high levels of autophagic degradative flux. The high LC3-II/LC3-I ratios observed following *Staphylococcus aureus* infection therefore suggest a combination of LC3 activation along with inhibition of degradation.

Surprisingly, *Salmonella* infection did not produce similar levels of LC3B-II. To further explore, we repeated the comparison but followed a *Salmonella*-optimized xenophagy protocol (see Methods) (36). However, using this second method, we also could not detect LC3B-II accumulation following infection with *Salmonella* (Figure 1B). Overall, xenophagy responses following *Staphylococcus aureus* and *Salmonella enterica sv. Typhimurium* infection were dramatically different.

Strain-dependent autophagy induction by *Staphylococcus aureus*

We next wanted to examine how the genotype of *Staphylococcus aureus* affects host cell autophagy responses. Previous studies have shown that the accessory gene regulator (*agr*) quorum sensing virulence system, which controls expression of factors like alpha haemolysin, was critical to induce autophagy (28,32,33). Here, we compared the experimental *Staphylococcus aureus* strains ATCC29213 (wildtype *agr*, methicillin-sensitive), NCTC8325 (wildtype *agr*, methicillin-resistant) and NRS144 (partial *agr*-deficient mutant of NCTC8325) (28). In addition, we studied a penicillin-, oxicillin-, ciprofloxacin-resistant strain isolated from an endo-tracheal aspirate that we previously characterised to represent clonal complex 8

(CC8) (*spa*-type t008) (37) and LF78, an epidemic strain of type EMRSA-15 with wide-antibiotic resistance (38). The three strains of wildtype virulent *Staphylococcus aureus* (ATCC29213, NCTC8325, and LF78) all strongly induced LC3B-II accumulation following infection of HeLa cells (Figure 1C). However, *agr*-mutant NRS144 only led to partial activation while the CC8 strain did not induce any detectable autophagy. These results confirm that the autophagic response depends on a functional *agr* and factors lacking in the CC8 strain.

Staphylococcus aureus infection generally produced high levels of LC3B-I lipidation and LC3B-II accumulation. Upon time-course analysis, we could detect maximal levels of LCB-II in HeLa cells at 3 hours of incubation with 100 MOI bacteria (Figure 1D). In this experiment, the cell population likely encounters multiple rounds of bacterial invasion, replication and further infection from new bacterial progeny along with parallel extracellular bacterial replication. To further characterize the dynamics, an additional timecourse was performed to study autophagy activation due to intracellular events. In this experiment, HeLa cells were incubated with 100 MOI *Staphylococcus aureus* for 1 hour after which gentamicin was added to inhibit growth of extracellular bacteria. With this protocol, LC3B-II levels peaked after 6 hours of infection. Therefore, after 1 hours of internalization, at least 5 additional hours is required for bacteria to transit through the initial phagosome and induce membrane damage to produce strong autophagy activation. These results highlight that levels of autophagy can increase depending on duration and extent of infection.

In light of the robust autophagy detected following *Staphylococcus* infection, we were puzzled by the negligible LC3-II accumulation observed upon *Salmonella* infection. Multiple studies have characterized the xenophagy defence mechanism for clearing *Salmonella* (2) (15,18,19,39) We wondered if poor autophagy activation by might explain why LC3 lipidation was not detected. To clarify, HeLa cells were infected with GFP-expressing *Salmonella enterica sv. Typhimurium* (using *Salmonella* optimized-protocol) and then immuno-stained

with anti-LC3B antibody. Using this imaging assay, we could confirm formation of LC3B(+) membranes elongating around or surrounding bacteria (Figure 2). To better understand the rate of xenophagy induction, we counted percentage of cells with autophagy membranes at different times of infection. While no puncta were detected within 20 min of infection, nearly 90% of cells exposed to *Salmonella* showed LC3B(+) membranes. The percentage of LC3B(+) cells rapidly decreased between 2-4 hours of infection suggestive of normal xenophagy flux. These results confirmed that *Salmonella* were able infect cells and trigger a rapid protective xenophagy response. The findings highlight that autophagy responses following *Staphylococcus* vs *Salmonella* infection were dramatically different. Lipidation and activation of LC3 in lysates was much more pronounced from the cell population following *Staphylococcus* infection.

p62/sequestosome1 recruitment during *Staphylococcus aureus* infection

To further investigate interactions with the autophagy pathway, we studied localization of the ubiquitin-binding adaptor, p62/SQSTM1. For this, we infected HeLa cells stably expressing GFP-p62 with NCTC8325 *Staphylococcus aureus*, which was detected by staining for protein A (Figure 3A). One clear effect was the formation of large-sized GFP-p62 structures in cells following infection with NCTC8325. However, while increases in GFP-p62 were obvious, we could not detect clear co-localisation between GFP-p62 and invading bacteria. These results suggest induction of ubiquitinated protein aggregates upon infection but raise questions regarding ubiquitin-mediated targeting of *Staphylococcus*. To clarify, we performed complementary experiments in which HeLa cells were infected with different *Staphylococcus strains* and endogenous p62 was detected by immunostaining. In this case, *Staphylococcus* were detected using Hoechst DNA stain (Figure 3B). With this second approach, we again found that invasion of cells with wildtype MRSA NCTC8325 led to formation of large sized p62 puncta that intermingle, but rarely co-localize, with bacteria. Interestingly, infection with CC8 or *agr*-mutant NRS144 also caused formation of

4

p62 puncta. However, these p62 puncta were generally of a smaller size range, resembling p62(+) formed after blocking the autophagy/lysosome pathway with chloroquine. Therefore, CC8 and *agr*-mutant *Staphylococcus* strains appear to lack key virulence factors required to promote strong accumulation of LC3B-II and p62 aggregates.

For comparison, we studied responses to *Salmonella* invasion. In this way, we could confirm robust formation of relatively smaller sized p62(+) structures in cells infected with *Salmonella* (Figure 3C). Many of the p62 structures were arranged laterally along, or occasionally, completely surrounding bacteria. By 1 hour after infection, p62(+) puncta could be detected in over 70% of infected cells and this percentage reduced over time, further suggesting normal degradative flux (Figure 3D). Collectively, these results are consistent with p62 serving as an adaptor for targeting ubiquitin-associated *Salmonella* to the xenophagy pathway. However, following infection with full virulence MRSA, distinctly enlarged p62 structures are formed, which may represent aggregates of ubiquitinated cellular proteins not associated with bacteria.

Intracellular *Staphylococcus aureus* promote non-canonical autophagosome formation

Staphylococcus have long been considered an extracellular pathogen but importance of the intracellular niche has become better appreciated (25). Therefore, we aimed to clarify that *Staphylococcus aureus* were promoting autophagosome formation following entry into the cellular endocytic system. Consistent with this notion, *Staphylococcus*-induced LCB-II formation was reduced when cytochalasin D was included to block bacterial internalization (40,41) (Figure 4A). As an alternative approach, we further confirmed that robust detection of intracellular *Staphylococcus* required permeablization of cell membranes before anti-protein A staining (Figure 4B,C).

Intracellular *Staphylococcus* clearly promoted large sized GFP-p62(+) and GFP-LCB(+) autophagosomes. Our other results on LC3B lipidation (Figure 1) suggested that *Staphylococcus* may activate autophagy while decreasing degradative capacity. To clarify, we conducted autophagy flux tests ± the lysosomal inhibitor, bafilomycin A1 (BafA1) (Figure 5A). We did not detect strong LC3B-II accumulation when BafA1 was added to inhibit the lysosome under basal conditions, consistent with low LC3B lipidation rates under full nutrient levels. In contrast, *Staphylococcus* infection promoted LC3B-II, suggestive of increased lipidation. Surprisingly, BafA1 suppressed *Staphylococcus*-dependent LC3B-II, which suggests that normally active lysosomes may be required to support autophagosome formation in this context. As parallel control, we confirmed that amino acid starvation promoted rapid canonical LC3B-II formation that was highly sensitive to lysosomal inhibition by BafA1.

We also investigated the relationship between autophagy flux and formation of large p62 membrane aggregates (Figure 5B). HeLa cells stably expressing GFP-LC3B showed small sized membrane structures in the basal full-nutrient state. These small sized canonical autophagosomes generally contained both GFP-LC3B and p62. Lysosomal inhibition with BafA1 did not lead to accumulation of autophagosomes, consistent with LC3B lipidation data from the parallel experiment above. In contrast, *Staphylococcus* infection led to large sized LC3B(+)/p62(+) aggregate structures (in 9.6% of infected cells). Formation of *Staphylococcus*-dependent LC3B(+)/p62(+) aggregates still occurred when the lysosome was inhibited with BafA1 (although at lower % of cells). Altogether, the data suggest that *Staphylococcus* infection leads to the production of non-canonical autophagosomes and this pathway does not reflect lysosomal inhibition.

Escape of *Staphylococcus aureus* from the lysosome-associated replication niche

Since the autophagy responses towards *Staphylococcus* vs. *Salmonella* infection were markedly different by LC3B and p62 readouts, we aimed to clarify how these pathogens interacted with lysosomes. HeLa cells in the basal state have small-sized lysosomes strongly staining for LAMP-2 (Figure 6A). Lysosome number and LAMP-2 staining greatly increased

5

when chloroquine was added to cells to block the autophagy/lysosome pathway. We examined lysosomal localisation of *Staphylococcus aureus* strains ATCC29213, NCTC8325, NRS144 and CC8 three hours post infection. Lysosomes became large and swollen following infection with ATCC29213 or NCTC8325 *Staphylococcus aureus*. Infection with these wildtype *Staphylococcus* strains led to high numbers of bacteria clustered in the cytoplasm with only a small fraction of bacteria enclosed by LAMP-2(+) membranes. In contrast, *agr*-deficient NRS144 were predominantly enclosed in LAMP-2(+) lysosomes with very few escaping to the cytoplasm. The CC8 strain showed an intermediate result, with fewer free bacteria in the cytosol. These results are consistent with the model in which invading *Staphylococcus* transit via the phagosome to an enlarged late-endosome/lysosome compartment. *Agr*-directed virulence factors in wildtype strains facilitate lysosomal membrane damage and bacterial escape to the cytoplasm, which is associated with LC3B activation and p62(+) ubiquitinated aggregates. Interestingly, the clinical CC8 MRSA isolate generates only very mild levels of LC3B accumulation, protein ubiquitination and lysosomal disruption, but was able to sustain a minimal level of human infection.

After characterizing escape of wildtype *Staphylococcus aureus* from degradative lysosomes, we aimed to confirm in parallel *Salmonella* transit from the lysosomal compartment. In HeLa cells infected with GFP-*Salmonella*, we could detect intracellular bacteria predominantly enclosed (or in very close proximity) with enlarged LAMP-2 (+) lysosomal membranes (Figure 6B). Consistent with previous reports (2), at early time points after infection (20 minutes, 1 hour post infection), there was low frequency of distended LAMP-2(+) membranes in *Salmonella* infected cells (Figure 6C). However, by two hours post infection, *Salmonella* infection led to formation of enlarged LAMP-2(+) compartments which remained strong even 5 hours post infection. Compared with fully virulent *Staphylococcus* infection, which led to bacteria mostly outside of LAMP-2 membranes, *Salmonella* were mostly all within LAMP(+) membranes. These

observations highlight how trafficking between these two pathogens via lysosomes is markedly different. *Staphylococcus aureus* rely on virulence factors to block transport and prevent lysosomal degradation to promote replication and eventual release into the cytoplasm. *Salmonella* are transported to lysosomal compartments within two hours post infection, via the xenophagy pathway, facilitating overall degradation of the bacteria.

To further explore *Staphylococcus aureus* and *Salmonella enterica sv. Typhimurium* interactions with the lysosome, we studied Galectin-3 (Gal3) puncta formation. Members of the Galectin family of beta-galactoside-binding proteins have served as useful tools to detect damage of endomembranes such as lysosomes. (42-45). Galectin-8 plays a critical role as receptor for targeting damaged SCV to the xenophagy pathway (46). As control, we first confirmed GFP-Gal3 puncta formation in HeLa cells treated with lysosomal stress compound, L-leucyl-L-leucine methyl ester (LLOME) (Figure 7A). We next tested infection with *Salmonella*, since these bacteria strongly co-localised with lysosomes within 2–5 hours post infection. Extensive GFP-Gal3 puncta of were found in almost all cells infected by *Salmonella enterica sv. Typhimurium* three hours post infection (Figure 7B). *Salmonella* showed extensive co-localisation with GFP-Gal3. By co-staining, we found clear co-localisation of endogenous LC3B(+) membranes on damaged lysosomes containing *Salmonella*. Therefore, our data are consistent with high levels of membrane damage on SCV to provide targeting signal for xenophagy. Overall, the LC3B(+) membrane signal in *Salmonella*-infected cells was even more prominent, going beyond areas of *Salmonella* or lysosomal damage. Therefore, there is strong activation of autophagosome formation, likely due to reactive oxygen species produced by NADPH oxidases upon *Salmonella* infection (47).

On the other hand, when we performed the parallel Gal3 experiment following MRSA infection, we observed entirely different trends (Figure 7C). Cells were infected with NCTC8325 for three hours (a time point with high levels of cytosolic bacteria). After NCTC8325 infection,

6

we surprisingly saw low levels of GFP-Gal3 puncta, suggesting little lysosome damage. To further evaluate this difference, we quantified GFP-Gal3 puncta following the same 5 hour timeframe for *Salmonella* versus MRSA infection (Figure 7D). *Salmonella enterica sv. Typhimurium* led to higher levels of lysosomal damage (>50 puncta / cell), similar to treatment with LLOME. These results suggest that MRSA carry virulence factors that allow bacterial replication and escape from lysosomes without high levels of membrane damage signals. MRSA therefore appear to have mechanisms for evasion of the Gal8 xenophagy defense pathway.

Host cell death following *Staphylococcus* and *Salmonella* infection

Through action of virulence factors such as alpha-haemolysin, *Staphylococcus aureus* can survive within a replicative niche to then escape into the cytoplasm (28,32) without signalling membrane damage. According to this model, we next characterized *Staphylococcus aureus* strains for efficiency to produce host cell death. We studied two different epithelial cells lines (standard HEK293 as compared to HEK293A, a more adherent subtype) as well as HeLa cells. These 3 cells types represent well-characterised experimental hosts for bacterial infection and autophagy. Host cells were infected with ATCC29213, CC8, NCTC8325 and EMRSA LF78 *Staphylococcus aureus* (Figure 8A). The 3 wildtype virulent *Staphylococcus aureus* types, ATCC29213, NCTC8325 and LF78, were potently cytotoxic for HEK and HeLa cells. In contrast, CC8 *Staphylococcus aureus* was non-cytotoxic. We further measured cytotoxicity in HeLa cells following infection with MRSA NCTC8325, *agr*-mutant NRS144 and CC8 *Staphylococcus aureus* (Figure 8B). We found a gradation of cytotoxicity. Surprisingly, CC8 *Staphylococcus aureus* was less cytotoxic than NRS144. Testing cytotoxity at different MOI (Figure 8C), we found that ATCC29213 showed higher cytotoxicity than NCTC8325, while NRS144 did not lead to cell killing, even at 500 MOI, indicating that this mutant detective strain was completely non-harmful to cells. These data highlight that expression of *agr*-dependent

virulence factors such as alpha haemolysin is essential for *Staphylococcus aureus* intracellular replication and host cell killing.

Above, we found that *Salmonella* infection led to extensive lysosomal damage, p62 recruitment and autophagosome formation consistent with xenophagy activation. Despite this anti-bacterial response, we wished to determine levels of cell death caused by *Salmonella* infection to complement our studies of MRSA. In macrophages, *Salmonella* derived lipopolysaccharide can induce caspase- and TLR4-dependent cell death (48-50). As such, we infected cell hosts HEK and HeLa with *Salmonella enterica sv. Typhimurium* and tested for viable cells that remained 72 hours post infection. We found that *Salmonella* infection led to potent killing of both HEK and HeLa cells (Figure 8D). Therefore, non-phagocytic cells are also susceptible to cytotoxic products produced from *Salmonella* infection.

Recruitment of the ULK1 complex to invading bacteria

ULK1 is a serine/threonine kinase that plays an essential role during the early steps of autophagosome biogenesis and we have previously characterized roles of this family of proteins in the regulation of canonical autophagy (51-53). In addition to standard autophagy, ULK1 complex has been shown to be important for promoting xenophagy to restrict *Salmonella* growth in host cells (54). On the other hand, roles for ULK1-dependent autophagy have also been demonstrated during *Brucella abortus* infection (55). In this case, inhibition of ULK1 function showed the opposite trend leading to reduced infection. Here, we aimed to further explore the potential of targeting ULK1 for the modulation of xenophagy. To study ULK1 function during formation of the double-bilayer autophagosome, we studied puncta containing ATG13, an essential component of the ULK1 complex that we previously characterized (51). ATG13 has been proposed to play a critical role for translocation of the ULK1 complex to membrane initiation sites of autophagy and mitophagy, potentially via specific lipid binding activity (56). As control, HeLa cells were starved of amino acid to stimulate canonical autophagy and stained for

endogenous ATG13 (Figure 9A). We could detect robust formation of approximately 10-20 finely-sized ATG13(+) puncta / cell within 1 hour of starvation. Next, we characterized translocation of the ULK1/ATG13 complex to invading *Salmonella* (Figure 9B). A small number of larger sized ATG13(+) puncta could be observed forming around GFP-*Salmonella* 1 hours post infection, an early timepoint consistent with peak association of LC3B on bacteria.

To compare, we examined ATG13(+) puncta following MRSA infection. As an alternative approach, we generated HeLa cells stably expressing GFP-ATG13 and first confirmed proper formation of starvation induced autophagosomes using this ectopic marker (Figure 9C), consistent with previous reports (56). To study ATG13 during MRSA-induced autophagy, we infected HeLa/GFP-ATG13 cells with NCTC8325 (Figure 9D). We could detect robust formation of GFP-ATG13(+) membrane structures localizing around clusters of *Staphylococcus* 3 hours post infection (Figure 9E). Together, these results suggest that the ULK1/ATG13 complex localizes to sites of *Salmonella* or *Staphylococcus* escape within hours of infection to drive formation of autophagosomes.

Inhibition of the ULK1-ATG13 pathway blocks *Staphylococcus aureus* infection

Since MRSA may subvert autophagy, we wished to determine if the ULK1/ATG13 pathway can be targeted during *Staphylococcus aureus* infection. We previously found that ULK1 and related family member ULK2 can both function for autophagy regulation (53). To achieve robust targeting of the ULK1/2 complex, we targeted the essential subunit ATG13 with the CRISPR-Cas9 system in HEK293A cells. As control, we confirmed that targeting of ATG13 strongly blocked starvation-induced autophagy flux as determined by lipidation of LC3B +/- BafA1 (Figure 10A). In addition, 293/ATG13-CRISPR cells were defective at LC3B(+) autophagosome formation following starvation (Figure 10B,C).

With strong targeting of ATG13, we next assessed effects on susceptibility to infection by *Staphylococcus aureus*. 293/ATG13-CRISPR or control cells were infected with varying MOI of MRSA (NCTC8325) and remaining viable cells were measured 72 hours post infection (Figure 10D). CRISPR targeting of ATG13 gave clear resistance to infection by NCTC8325. Therefore, inhibition of the ULK1/ATG13 autophagy complex appears to suppress extent to which *Staphylococcus aureus* infect and kill cells. To compare, we also tested how ATG13 targeting affected infection by *Salmonella*. Although wildtype 293A cells show clear levels of cell death following *Salmonella enterica sv. Typhimurium* infection, 293/ATG13-CRISPR cells were more sensitive (Figure 10E), particularly when measuring viable cells remaining 24 hours post-infection. This result further suggests that while the ULK1/ATG13 complex localizes to both invading *Staphylococcus aureus* and *Salmonella*, autophagy plays opposite roles in the interaction with these pathogens.

To further explore inhibition of xenophagy, HeLa cells were generated stably expressing shRNA towards ULK1 (Figure 11A). Strong knockdown of ULK1 was sufficient to reduce starvation induced autophagy flux in the LC3B lipidation assay. LC3B-II generation following MRSA infection was also inhibited by ULK1 knockdown. To note, partial autophagy inhibition observed here despite strong ULK1 knockdown may reflect residual ULK2 function in HeLa cells. HeLa/shULK1 cells showed clear resistance to MRSA-induced cell death (Figure 11B). Conversely, HeLa/shULK1 cells were more sensitive to *Salmonella*-induced cell death (Figure 11C).

Several ATP-pocket binding ULK1/ULK2 inhibitors have been developed that block autophagy, for example, MRT68921 and SBI-0206965, bringing the field closer towards targeting this pathway as a therapeutic (57-59). Here, we tested ULK1/2 inhibitors for their ability to modulate cell death following MRSA infection. Both MRT68921 and SBI-0206965 at high (10 µM) or low (1µM) concentration were able to improve cell viability after infection with MRSA (NCTC8325) (Figure 11D). Incubation with 10 µM MRT68921 for the 48 hour experiment led to some mild background

8

cytotoxicity so this drug at 1 µM provided better rescue following bacterial infection. To complement this analysis, we tested effects of MRT68921 and SBI-0206965 on cell viability after *Salmonella enterica sv. Typhimurium* infection. Both of these ULK1/2 inhibitors led to significantly higher amounts of cell death after *Salmonella* infection (Figure 11E). Therefore, pharmacological inhibition of the ULK1/2 pathway had opposite effects on cell viability after *Staphylococcus* vs *Salmonella* infection. Since ULK1/2 inhibitors appeared to block *Staphylococcus aureus* infection of mammalian cells, we wanted to check that ULK1 inhibitors were not directly affecting bacteria. In this way, we confirmed that both ULK1/2 inhibitors (10 µM) did not have any effect on *Staphylococcus* or *Salmonella* in liquid culture growth assays (Figure 11F). In contrast, gentamicin completely inhibited growth of both these types of bacteria.

Next, to clarify how ULK1/2 inhibitors rescue cells in MRSA experiments, we confirmed that SBI-0206965 and MRT68921 robustly inhibited autophagy in our experimental cell systems. Both compounds at 10 µM blocked formation of starvation-dependent LC3B(+) autophagosomes (Figure 11G,H). To further clarify effects of ULK1/2 inhibitors on bacteria-induced autophagy, we studied p62 aggregate formation. HeLa/GFP-p62 cells treated with MRT68921 or SBI-0206965 were infected with NCTC8325. Indeed, treatment with MRT68921 reduced formation of large p62(+) aggregate structures following infection by NCTC8325 (Figure 11I,J). Note, we still detected smaller-sized p62 puncta without any associated NCTC8325 in the presence of MRT68921. On the other hand, treatment with SBI-0206965 inhibited both large p62 aggregates and smaller p62 puncta. Interestingly, invading MRSA were still observed within infected cells treated with MRT68921 or SBI-0206965. Therefore, ULK1/2 inhibitors blocked MRSA-induced p62 aggregates and cell death, but not initial stages of bacterial infection.

Lastly, we clarified roles for autophagy during infection, since *Staphylococcus aureus* still appeared to invade cells even with ULK1 inhibition. For this, we measured levels of intracellular *Staphylococcus aureus* (colony forming units (CFU)) within cell lysates. HEK293A cells were infected with NCTC8325 in the presence of MRT68921 (1 µM) or SBI-0206965 (10 µM). After one hour of infection, gentamicin was added to inactivate extracellular NCTC8325 and host cells were lysed at timepoints thereafter to monitor replication of bacteria that invaded cells. In cells without ULK1/2 inhibitor, *Staphylococcus aureus* CFU increased rapidly within 3-6 hours after addition of gentamicin, leading to death of HEK293A hosts within 24 hours (Figure 11K). At 3 hours post infection (without ULK inhibitors), we detected 2.7×10^6 CFU/ mL in cell lysates. This titre corresponds to ~150% of the CFU used to inoculate each well of host cells. Assuming bacterial doubling time of 0.5 hrs, we estimate ~2.3% of *Staphylococcus aureus* (150% / 2^6) were able to invade and proliferate within host cells within 3 hours of infection. Strikingly, treatment with either MRT68921 or SBI-0206965 almost completely inhibited MRSA intracellular replication. Host cells maintained health 24 to 48 (data not shown) hours after infection with the addition of ULK1 inhibitors. Therefore, blocking ULK1-dependent autophagy suppresses overall *Staphylococcus aureus* infection.

Discussion

Staphylococcus aureus infection remains to be a leading cause of human bacterial infections world-wide and presents a major issue for both hospital and community health care contexts (24). A further complication comes from the rise of antibiotic resistance and strains of MRSA that resist many first lines of treatment. Despite the importance of *Staphylococcus* as a pathogen, roles of host cell autophagy during the infection process *in vitro* and *in vivo* remain controversial (28,60,61) and less well-understood as compared with other bacteria such as *Salmonella*. Here, we aimed to clarify the role of autophagy during *Staphylococcus* infection of non-phagocytic cell types such as HEK293 and HeLa.

Interaction of *Staphylococcus aureus* with the host cell autophagy pathway

We found strong indications of autophagy such as accumulation of the lipidated, activated form of the ATG8 member, LC3B, upon infection with

9

wildtype, fully-virulent strains of *Staphylococcus aureus* carrying an active *agr* quorum-sensing system. Our observations of robust LC3 lipidation are consistent with previous data documenting strong phenotypes on this autophagosomal marker during *Staphylococcus* infection (28,32,34,61). Surprisingly, lipidation of LC3B after *Salmonella* infection was barely detectable. Moreover, we found strong accumulation of p62-positive aggregates in cells infected with *Staphylococcus aureus*, suggestive of hyperactive protein ubiquitination or defective clearance. Interestingly, there was negligible or partial co-localization of p62 aggregates on *Staphylococcus,* which suggests that the ubiquitinated targets may be predominantly host cell proteins. Formation of the p62 aggregate phenotype was dependent on function of the *agr*-system, consistent with other work demonstrating the importance of *Staphylococcus* virulence factors such as alpha-haemolysin for interaction with the autophagy pathway (28,32,33,61).

We were also intrigued since a clinical *Staphylococcus* isolate from an endo-tracheal aspirate that we previously genotyped as CC8 (37) did not induce p62 aggregates or other markers of autophagy and infection-related cell death. There has been another report suggesting p62-mediated targeting of ubiquitinated cytosolic *Staphylococcus aureus* using the SH1000 strain which is also CC8 (34). *Staphylococcus aureus* SH1000 has been shown to carry less *agr*-dependent membrane lytic activity, resulting in lower rates of death in infected host cells (61). Although more representative strains should be investigated, our data are consistent with lower levels of p62-dependent autophagy and lower levels of proliferative cellular infection with CC8 *Staphylococcus aureus*. Indeed, wildtype virulent *Staphylococcus aureus* strains appeared to extensively escape from their lysosome-associated replicative niche into the cytoplasm, but *agr*-mutant or CC8 strains showed lower levels of this behaviour. We had previously used Gal-3 as a cellular probe to detect lysosome membrane damage following treatment with the cancer chemotherapeutic (and anti-malarial) compound chloroquine (42). A related protein Gal-8 has been shown to detect membrane damage to mount xenophagy for the restriction of

Salmonella infection (46). Members of the galectin family have multiple mechanisms to coordinate autophagy regulation (62,63). Surprisingly, we *Staphylococcus aureus* appeared to escape from the lysosome without strong Gal-3 recruitment, in contrast with membrane disruption events during *Salmonella* infection. Therefore, *Staphylococcus aureus* may have acquired virulence factors such as alpha-haemolysin that can perturb membrane compartments during the infection life cycle without triggering innate anti-bacterial pathways.

ULK1 inhibition as a strategy to block *Staphylococcus aureus* infection

We aimed to explore the potential of targeting autophagy during bacterial infection. In particular, we have had long-standing interest in the ULK1 autophagy complex which functions at an early regulatory checkpoint during autophagosome biogenesis (51-53). Several different ULK1 small molecule inhibitors have been developed that target the ATP-binding pocket of the kinase domain as a strategy to inhibit autophagy (58,64). Here, we could show that the ULK1 complex (via ATG13) localizes to sites of either *Salmonella* or *Staphylococcus* invasion in the cytoplasm where the complex might promote autophagosome formation around bacteria. Previously, others have also shown ULK1 or members of the WIPI PI3P-binding protein family co-localizing on cytosolic *Salmonella* or *Staphylococcus* (33,54,65,66). Interestingly, genetic targeting of the ULK1-ATG13 pathway blocked autophagy and prevented the ability of *Staphylococcus aureus* infection to progress towards cell death. These data are consistent with a role for autophagy in the generation of a replicative niche to support *Staphylococcus aureus* infection, originally described by Krut and colleagues (28). Conversely, ULK1-ATG13 targeting produced the opposite effect and sensitized cells to *Salmonella*-infection cytotoxicity. This effect is consistent with the current model featuring anti-bacterial autophagy/xenophagy during *Salmonella* infection (2,15,19,54,66). Importantly, both ULK1 inhibitors that we tested (MRT68921 and SBI-0206965) (57,58) could robustly inhibit *Staphylococcus* intracellular

10

replication and host cell death. Previously, autophagy-dependent *Staphylococcus* infection was blocked via the PI3K inhibitor wortmannin, which would widely affect other cellular pathways (28). Cells treated with ULK1 inhibitors still showed substantial numbers of *Staphylococcus* invading the cytoplasm. Since bacterial titres in cell lysates in these cases were dramatically low, an autophagy-dependent niche appears to be essential for intracellular replication.

Our results highlight the potential of autophagy targets like ULK1 to inhibit the formation of intracellular replication sites during bacterial infection. ULK1 inhibitors were effective at preventing *Staphylococcus* infection of non-professional phagocytic cell lines and it will be useful to test more broadly, for example, in other physiological cell hosts like macrophages (67). The ability of *Staphylococcus aureus* to reside within an intracellular niche provides a basis for antibiotic evasion and persistence of infection (26). Autophagy inhibition to block infection might be suitable for other bacteria dependent on formation of intracellular replication compartments such as *Brucella abortus* and *Coxiella burnetii* (55,68-70). Our results further highlight that autophagy can play opposite roles depending on the pathogen since inhibition of ULK1 makes cells hypersensitive to other bacteria such as *Salmonella*.

Experimental Procedures

Cell culture: HEK293A and HeLa cells were maintained in DMEM with 4.5g/L glucose (Lonza #BE12-614F) supplemented with 10% fetal bovine serum (FBS) (Labtech #FCS-SA), 4mM L-Glutamine (Lonza #BE17-605E), and 100U/mL Penicillin/Streptomycin (Lonza #DE17-602E). Where indicated, HeLa cells were transduced with retrovirus carrying pMXs-IP-GFP-hATG13 (71) or pMXs-puro-GFP-p62 (72) and selected under puromycin. HEK293A cells with CRISPR-Cas9 targeting of ATG13 were generated using the lentiCRISPR v2 (one-vector) system (73). Guide RNA sequences for ATG13 from the human GeCKO library (74) were cloned into lentiCRISPR v2 and screened for ATG13 targeting efficiency by immunoblot. The gRNA used throughout this study was: ATG13-

HGLibA_03468 corresponding to GACTGTCCAAGTGATTGTCC. After transduction of cells with lentivirus, puromycin selection was performed and isolated clones were confirmed for targeting efficiency by immunoblot. All results with ATG13 CRISPR targeting were confirmed via independent experiments using pools of CRISPR-targeted cells analysed 1-2 passage immediately after puromycin selection. Alternatively, ULK1 knockdown was performed using pLKO.1 shRNA (TRCN0000000835, Broad Institute Genetic Perturbation Platform, obtained from Open Biosystems / Dharmacon). As autophagy control, cells were starved of amino acid (and serum) in Earle's balanced salt solution (EBSS) (52) or treated with chloroquine (42) as described.

Bacterial infection: Strains of *Staphylococcus aureus* used include: ATCC29213 (Methicillin-Sensitive, *agr*-wildtype); NCTC8325 (Methicillin-Resistant, MRSA) (obtained from Public Health England, National Collection of Type Cultures); epidemic MRSA strain LF78 (38); NRS144 (*agr*-mutant); and clonal complex 8 Staphylococcus aureus (37). *Salmonella enterica sv. Typhimurium* (NCTC 13347 (SL 1344)) was obtained from Public Health England, National Collection of Type Cultures. All *Staphylococcus aureus* strains were maintained on mannitol salt agar (MSA) plates (OXOID 1106008) or tryptic soy broth (TSB) (Fluka analytical, 22092) in liquid cultures. *Salmonella enterica* were grown on nutrient agar plates (OXOID 1655783) and TSB liquid cultures. Where indicated, *Salmonella* were transformed by electroporation with GFP expressing plasmid using standard methods followed by selection with ampicillin. We subcloned EGFP as a PCR fragment via sites HindIII-EcoRI into the backbone from pGFPuv (Clontech #632312).

Staphylococcus aureus infection were performed based on a previously reported protocol (28). Overnight cultures in TSB were diluted 1:100 on the day of the experiment and grown until mid-logarithmic phase (OD600 = 0.3 ± 0.05). Based on actual OD, bacteria pellets were adjusted to varying volumes in Pen/Strep-free DMEM to

yield (typically) 100 multiplicity of infection (MOI).

Host cells (HEK293A or HeLa) were seeded in 12 well plates for immunoblotting or on poly-D-lysine coated coverslips in 24 well plates in Pen/Strep-free DMEM/10% FBS. The following day, *Staphylococcus* /DMEM suspension was added to host cells (100μl to each well of 12-well plate containing 1 ml media; 50μl to each well of 24-well plate containing 0.5 ml media) and incubated for 1 hour at 37°C. After this hour, gentamicin (Lonza, 17-519L) was added to 0.05 mg/ml final (where indicated) and cells further incubated at 37°C for varying times before cell lysis or fixation.

We infected cells with *Salmonella* using a protocol previously reported for xenophagy experiments (36). Overnight cultures of *Salmonella enterica sv. Typhimurium* (NCTC 13347) in TSB were diluted 1:33 on the day of the experiment in 10 mL of TSB broth and grown for 3 hours with shaking resulting in OD600 = 1.2–1.5 (corresponding to ~ 1 * 10exp8 bacteria/ml). This culture of *Salmonella* was further diluted 1:100 in Pen/Strep-free DMEM/ 10% FBS to generate a *Salmonella* stock culture. For infection, medium was first removed from host cells (plated as above) and replaced with 1ml (for 12-well plate) or 0.5 ml for (24-well plate) diluted *Salmonella* stock culture at time=0. After incubation for 20 minutes at 37°C, media were changed into fresh Pen/Strep-free DMEM/10% FBS and further incubated at 37°C for 30 minutes. Following, media were further exchanged with Pen/Strep-free DMEM/ 10% FBS containing gentamicin (0.05mg/ml) and incubated further for varying amounts of time.

Immunoblot analysis: Cell lysates were prepared and analysed using on 4-12% NuPAGE gels (for LC3B) or 10% hand-poured Bis-Tris gels in MES running buffer (Thermo Fisher scientific) as described previously (52,53). Membranes were stained using the following antibodies. LC3B: clone 5F10 (Nanotools #0231-100); ULK1-D8H5 (Cell signalling 8054); ATG13-D4P1K (Cell signalling 13273); Actin: Ab-5 (BD Bioscience # 612656). Detection was via anti-mouse or anti-rabbit Dylight-coupled secondary antibodies and Licor Odyssey infra-red scanning.

Microscopy: After treatments, cells were fixed and stained using the following antibodies: anti-p62/SQSTM1 (BD Transduction Laboratories mouse anti-p62/lck ligand #610832); LAMP-2 (BD Transduction Laboratories mouse anti-human CD107b), LC3B (Cell signalling, #2775) or ATG13-D4P1K (Cell signalling, #13273). In some cases, *Staphylococcus aureus* were stained with anti-protein A (Sigma, P2921) or Hoechst 33342. In some cases, *Salmonella* were stained with DAPI.

For Gal-3 puncta tests, HeLa cells plated on glass coverslips were transfected with pEGFP-hGal3 (Addgene: 73080) (45) using Lipofectamine 2000 according to standard protocols, as we have previously reported (42). After 24 hours of transfection, cells were used for experiments. Cell images were captured by confocal microscopy (Figures 2,3,6,7,9-11: Leica, TCS SP5, HCX PL APO CS-63x-1.4NA objective and HyD GaAsP detection; Figures 4,5: Zeiss LSM 710, Plan-Apochromat 63x-1.4NA objective). Puncta/cell were quantified from confocal scans (or directly by epifluorescent imaging), depending on the marker.

Cell killing by bacterial infection: At varying times (24-72 hrs as indicated) after infection, viable cells remaining attached to the culture dish were fixed with 10% formalin / PBS, washed in PBS/methanol (1:1) and then stained with dilute Giemsa stain (Fluka BCBK8476V). Plates were washed and then dried. To quantify Giemsa stain, dyed cellular material were solubilized in 30% acetic acid/water and measured at Abs 560nm, as we and others have previously described (42,75).

Staphylococcus intracellular replication: Infected host cells were washed with PBS once and lysed in 0.05% Triton X-100/ PBS. Lysates were diluted with PBS and plated on MSA plates. Overnight colonies were counted and normalized CFU (colony forming units) was calculated.

ULK1 inhibitors: We obtained MRT68921 from B. Saxty, Medical Research Council UK / LifeArc (58). ULK1 inhibitor SBI-0206965 was synthesized according to the reported scheme (57). The final compound was purified by HPLC and confirmed by NMR analysis followed by tests in cells described here.

12

Statistics: Quantitative data were managed using GraphPad Prism and analysed using unpaired T-test (for 2-way comparisons) or one-way ANOVA with Tukey post-test (multiple comparisons) as appropriate.

Acknowledgements

Conflicts of interest

The authors have no competing financial interests.

References

1. Yu, L., Chen, Y., and Tooze, S. A. (2018) Autophagy pathway: Cellular and molecular mechanisms. *Autophagy* **14**, 207-215
2. Birmingham, C. L., Smith, A. C., Bakowski, M. A., Yoshimori, T., and Brumell, J. H. (2006) Autophagy controls Salmonella infection in response to damage to the Salmonella-containing vacuole. *J Biol Chem* **281**, 11374-11383
3. Gutierrez, M. G., Master, S. S., Singh, S. B., Taylor, G. A., Colombo, M. I., and Deretic, V. (2004) Autophagy is a defense mechanism inhibiting BCG and Mycobacterium tuberculosis survival in infected macrophages. *Cell* **119**, 753-766
4. Zhao, Z., Fux, B., Goodwin, M., Dunay, I. R., Strong, D., Miller, B. C., Cadwell, K., Delgado, M. A., Ponpuak, M., Green, K. G., Schmidt, R. E., Mizushima, N., Deretic, V., Sibley, L. D., and Virgin, H. W. (2008) Autophagosome-independent essential function for the autophagy protein Atg5 in cellular immunity to intracellular pathogens. *Cell Host Microbe* **4**, 458-469
5. Py, B. F., Lipinski, M. M., and Yuan, J. (2007) Autophagy limits Listeria monocytogenes intracellular growth in the early phase of primary infection. *Autophagy* **3**, 117-125
6. Nakagawa, I., Amano, A., Mizushima, N., Yamamoto, A., Yamaguchi, H., Kamimoto, T., Nara, A., Funao, J., Nakata, M., Tsuda, K., Hamada, S., and Yoshimori, T. (2004) Autophagy defends cells against invading group A Streptococcus. *Science* **306**, 1037-1040
7. Huett, A., Heath, R. J., Begun, J., Sassi, S. O., Baxt, L. A., Vyas, J. M., Goldberg, M. B., and Xavier, R. J. (2012) The LRR and RING domain protein LRSAM1 is an E3 ligase crucial for ubiquitin-dependent autophagy of intracellular Salmonella Typhimurium. *Cell Host Microbe* **12**, 778-790
8. Noad, J., von der Malsburg, A., Pathe, C., Michel, M. A., Komander, D., and Randow, F. (2017) LUBAC-synthesized linear ubiquitin chains restrict cytosol-invading bacteria by activating autophagy and NF-kappaB. *Nature microbiology* **2**, 17063
9. Polajnar, M., Dietz, M. S., Heilemann, M., and Behrends, C. (2017) Expanding the host cell ubiquitylation machinery targeting cytosolic Salmonella. *EMBO Rep* **18**, 1572-1585
10. van Wijk, S. J., Fiskin, E., Putyrski, M., Pampaloni, F., Hou, J., Wild, P., Kensche, T., Grecco, H. E., Bastiaens, P., and Dikic, I. (2012) Fluorescence-based sensors to monitor localization and functions of linear and K63-linked ubiquitin chains in cells. *Mol Cell* **47**, 797-809
11. Fujita, N., Morita, E., Itoh, T., Tanaka, A., Nakaoka, M., Osada, Y., Umemoto, T., Saitoh, T., Nakatogawa, H., Kobayashi, S., Haraguchi, T., Guan, J. L., Iwai, K., Tokunaga, F., Saito, K., Ishibashi, K., Akira, S., Fukuda, M., Noda, T., and Yoshimori, T. (2013) Recruitment of the autophagic machinery to endosomes during infection is mediated by ubiquitin. *J Cell Biol* **203**, 115-128
12. Fiskin, E., Bionda, T., Dikic, I., and Behrends, C. (2016) Global Analysis of Host and Bacterial Ubiquitinome in Response to Salmonella Typhimurium Infection. *Mol Cell* **62**, 967-981
13. Perrin, A. J., Jiang, X., Birmingham, C. L., So, N. S., and Brumell, J. H. (2004) Recognition of bacteria in the cytosol of Mammalian cells by the ubiquitin system. *Curr Biol* **14**, 806-811
14. Wang, L., Yan, J., Niu, H., Huang, R., and Wu, S. (2018) Autophagy and Ubiquitination in Salmonella Infection and the Related Inflammatory Responses. *Front Cell Infect Microbiol* **8**, 78
15. Zheng, Y. T., Shahnazari, S., Brech, A., Lamark, T., Johansen, T., and Brumell, J. H. (2009) The adaptor protein p62/SQSTM1 targets invading bacteria to the autophagy pathway. *J Immunol* **183**, 5909-5916
16. von Muhlinen, N., Akutsu, M., Ravenhill, B. J., Foeglein, A., Bloor, S., Rutherford, T. J., Freund, S. M., Komander, D., and Randow, F. (2012) LC3C, bound selectively by a noncanonical LIR motif in NDP52, is required for antibacterial autophagy. *Mol Cell* **48**, 329-342

14

17.   Ivanov, S., and Roy, C. R. (2009) NDP52: the missing link between ubiquitinated bacteria and autophagy. *Nat Immunol* **10**, 1137-1139

18.   Thurston, T. L., Ryzhakov, G., Bloor, S., von Muhlinen, N., and Randow, F. (2009) The TBK1 adaptor and autophagy receptor NDP52 restricts the proliferation of ubiquitin-coated bacteria. *Nat Immunol* **10**, 1215-1221

19.   Wild, P., Farhan, H., McEwan, D. G., Wagner, S., Rogov, V. V., Brady, N. R., Richter, B., Korac, J., Waidmann, O., Choudhary, C., Dotsch, V., Bumann, D., and Dikic, I. (2011) Phosphorylation of the autophagy receptor optineurin restricts Salmonella growth. *Science* **333**, 228-233

20.   Cemma, M., Kim, P. K., and Brumell, J. H. (2011) The ubiquitin-binding adaptor proteins p62/SQSTM1 and NDP52 are recruited independently to bacteria-associated microdomains to target Salmonella to the autophagy pathway. *Autophagy* **7**, 341-345

21.   Tumbarello, D. A., Manna, P. T., Allen, M., Bycroft, M., Arden, S. D., Kendrick-Jones, J., and Buss, F. (2015) The Autophagy Receptor TAX1BP1 and the Molecular Motor Myosin VI Are Required for Clearance of Salmonella Typhimurium by Autophagy. *PLoS Pathog* **11**, e1005174

22.   Shahnazari, S., and Brumell, J. H. (2011) Mechanisms and consequences of bacterial targeting by the autophagy pathway. *Curr Opin Microbiol* **14**, 68-75

23.   Yuk, J. M., Yoshimori, T., and Jo, E. K. (2012) Autophagy and bacterial infectious diseases. *Exp Mol Med* **44**, 99-108

24.   Turner, N. A., Sharma-Kuinkel, B. K., Maskarinec, S. A., Eichenberger, E. M., Shah, P. P., Carugati, M., Holland, T. L., and Fowler, V. G., Jr. (2019) Methicillin-resistant Staphylococcus aureus: an overview of basic and clinical research. *Nat Rev Microbiol* **17**, 203-218

25.   Moldovan, A., and Fraunholz, M. J. (2019) In or out: Phagosomal escape of Staphylococcus aureus. *Cell Microbiol* **21**, e12997

26.   Lehar, S. M., Pillow, T., Xu, M., Staben, L., Kajihara, K. K., Vandlen, R., DePalatis, L., Raab, H., Hazenbos, W. L., Morisaki, J. H., Kim, J., Park, S., Darwish, M., Lee, B. C., Hernandez, H., Loyet, K. M., Lupardus, P., Fong, R., Yan, D., Chalouni, C., Luis, E., Khalfin, Y., Plise, E., Cheong, J., Lyssikatos, J. P., Strandh, M., Koefoed, K., Andersen, P. S., Flygare, J. A., Wah Tan, M., Brown, E. J., and Mariathasan, S. (2015) Novel antibody-antibiotic conjugate eliminates intracellular S. aureus. *Nature* **527**, 323-328

27.   Schroder, A., Kland, R., Peschel, A., von Eiff, C., and Aepfelbacher, M. (2006) Live cell imaging of phagosome maturation in Staphylococcus aureus infected human endothelial cells: small colony variants are able to survive in lysosomes. *Med Microbiol Immunol* **195**, 185-194

28.   Schnaith, A., Kashkar, H., Leggio, S. A., Addicks, K., Kronke, M., and Krut, O. (2007) Staphylococcus aureus subvert autophagy for induction of caspase-independent host cell death. *J Biol Chem* **282**, 2695-2706

29.   Lopez de Armentia, M. M., Gauron, M. C., and Colombo, M. I. (2017) Staphylococcus aureus Alpha-Toxin Induces the Formation of Dynamic Tubules Labeled with LC3 within Host Cells in a Rab7 and Rab1b-Dependent Manner. *Front Cell Infect Microbiol* **7**, 431

30.   Grosz, M., Kolter, J., Paprotka, K., Winkler, A. C., Schafer, D., Chatterjee, S. S., Geiger, T., Wolz, C., Ohlsen, K., Otto, M., Rudel, T., Sinha, B., and Fraunholz, M. (2014) Cytoplasmic replication of Staphylococcus aureus upon phagosomal escape triggered by phenol-soluble modulin alpha. *Cell Microbiol* **16**, 451-465

31.   Blattner, S., Das, S., Paprotka, K., Eilers, U., Krischke, M., Kretschmer, D., Remmele, C. W., Dittrich, M., Muller, T., Schuelein-Voelk, C., Hertlein, T., Mueller, M. J., Huettel, B., Reinhardt, R., Ohlsen, K., Rudel, T., and Fraunholz, M. J. (2016) Staphylococcus aureus Exploits a Non-ribosomal Cyclic Dipeptide to Modulate Survival within Epithelial Cells and Phagocytes. *PLoS Pathog* **12**, e1005857

32.   Mestre, M. B., Fader, C. M., Sola, C., and Colombo, M. I. (2010) Alpha-hemolysin is required for the activation of the autophagic pathway in Staphylococcus aureus-infected cells. *Autophagy* **6**, 110-125

33.   Mauthe, M., Yu, W., Krut, O., Kronke, M., Gotz, F., Robenek, H., and Proikas-Cezanne, T. (2012) WIPI-1 Positive Autophagosome-Like Vesicles Entrap Pathogenic Staphylococcus aureus for Lysosomal Degradation. *Int J Cell Biol* **2012**, 179207

34.   Neumann, Y., Bruns, S. A., Rohde, M., Prajsnar, T. K., Foster, S. J., and Schmitz, I. (2016) Intracellular Staphylococcus aureus eludes selective autophagy by activating a host cell kinase. *Autophagy* **12**, 2069-2084

35.   Kabeya, Y., Mizushima, N., Ueno, T., Yamamoto, A., Kirisako, T., Noda, T., Kominami, E., Ohsumi, Y., and Yoshimori, T. (2000) LC3, a mammalian homologue of yeast Apg8p, is localized in autophagosome membranes after processing. *The EMBO journal* **19**, 5720-5728

36.   Huett, A., Ng, A., Cao, Z., Kuballa, P., Komatsu, M., Daly, M. J., Podolsky, D. K., and Xavier, R. J. (2009) A novel hybrid yeast-human network analysis reveals an essential role for FNBP1L in antibacterial autophagy. *J Immunol* **182**, 4917-4930

37.   Sangal, V., Girvan, E. K., Jadhav, S., Lawes, T., Robb, A., Vali, L., Edwards, G. F., Yu, J., and Gould, I. M. (2012) Impacts of a long-term programme of active surveillance and chlorhexidine baths on the clinical and molecular epidemiology of meticillin-resistant Staphylococcus aureus (MRSA) in an Intensive Care Unit in Scotland. *Int J Antimicrob Agents* **40**, 323-331

38.   Raghukumar, R., Vali, L., Watson, D., Fearnley, J., and Seidel, V. (2010) Antimethicillin-resistant Staphylococcus aureus (MRSA) activity of 'pacific propolis' and isolated prenylflavanones. *Phytotherapy research : PTR* **24**, 1181-1187

39.   Verlhac, P., Gregoire, I. P., Azocar, O., Petkova, D. S., Baguet, J., Viret, C., and Faure, M. (2015) Autophagy receptor NDP52 regulates pathogen-containing autophagosome maturation. *Cell Host Microbe* **17**, 515-525

40.   Agerer, F., Michel, A., Ohlsen, K., and Hauck, C. R. (2003) Integrin-mediated invasion of Staphylococcus aureus into human cells requires Src family protein-tyrosine kinases. *J Biol Chem* **278**, 42524-42531

41.   Wells, C. L., van de Westerlo, E. M., Jechorek, R. P., Haines, H. M., and Erlandsen, S. L. (1998) Cytochalasin-induced actin disruption of polarized enterocytes can augment internalization of bacteria. *Infection and immunity* **66**, 2410-2419

42.   Gallagher, L. E., Radhi, O. A., Abdullah, M. O., McCluskey, A. G., Boyd, M., and Chan, E. Y. W. (2017) Lysosomotropism depends on glucose: a chloroquine resistance mechanism. *Cell death & disease* **8**, e3014

43.   Paz, I., Sachse, M., Dupont, N., Mounier, J., Cederfur, C., Enninga, J., Leffler, H., Poirier, F., Prevost, M. C., Lafont, F., and Sansonetti, P. (2010) Galectin-3, a marker for vacuole lysis by invasive pathogens. *Cell Microbiol* **12**, 530-544

44.   Aits, S., Kricker, J., Liu, B., Ellegaard, A. M., Hamalisto, S., Tvingsholm, S., Corcelle-Termeau, E., Hogh, S., Farkas, T., Holm Jonassen, A., Gromova, I., Mortensen, M., and Jaattela, M. (2015) Sensitive detection of lysosomal membrane permeabilization by lysosomal galectin puncta assay. *Autophagy* **11**, 1408-1424

45.   Maejima, I., Takahashi, A., Omori, H., Kimura, T., Takabatake, Y., Saitoh, T., Yamamoto, A., Hamasaki, M., Noda, T., Isaka, Y., and Yoshimori, T. (2013) Autophagy sequesters damaged lysosomes to control lysosomal biogenesis and kidney injury. *The EMBO journal* **32**, 2336-2347

46.   Thurston, T. L., Wandel, M. P., von Muhlinen, N., Foeglein, A., and Randow, F. (2012) Galectin 8 targets damaged vesicles for autophagy to defend cells against bacterial invasion. *Nature* **482**, 414-418

47.   Huang, J., Canadien, V., Lam, G. Y., Steinberg, B. E., Dinauer, M. C., Magalhaes, M. A., Glogauer, M., Grinstein, S., and Brumell, J. H. (2009) Activation of antibacterial autophagy by NADPH oxidases. *Proc Natl Acad Sci U S A* **106**, 6226-6231

48.   Thurston, T. L., Matthews, S. A., Jennings, E., Alix, E., Shao, F., Shenoy, A. R., Birrell, M. A., and Holden, D. W. (2016) Growth inhibition of cytosolic Salmonella by caspase-1 and caspase-11 precedes host cell death. *Nat Commun* **7**, 13292

49.   Hagar, J. A., Powell, D. A., Aachoui, Y., Ernst, R. K., and Miao, E. A. (2013) Cytoplasmic LPS activates caspase-11: implications in TLR4-independent endotoxic shock. *Science* **341**, 1250-1253

50.   Hsu, L. C., Park, J. M., Zhang, K., Luo, J. L., Maeda, S., Kaufman, R. J., Eckmann, L., Guiney, D. G., and Karin, M. (2004) The protein kinase PKR is required for macrophage apoptosis after activation of Toll-like receptor 4. *Nature* **428**, 341-345

51.   Chan, E. Y., Longatti, A., McKnight, N. C., and Tooze, S. A. (2009) Kinase-inactivated ULK proteins inhibit autophagy via their conserved C-terminal domains using an Atg13-independent mechanism. *Mol Cell Biol* **29**, 157-171

52.   Nwadike, C., Williamson, L. E., Gallagher, L. E., Guan, J. L., and Chan, E. Y. W. (2018) AMPK Inhibits ULK1-Dependent Autophagosome Formation and Lysosomal Acidification via Distinct Mechanisms. *Mol Cell Biol* **38**

53.   McAlpine, F., Williamson, L. E., Tooze, S. A., and Chan, E. Y. (2013) Regulation of nutrient-sensitive autophagy by uncoordinated 51-like kinases 1 and 2. *Autophagy* **9**, 361-373

54.   Kageyama, S., Omori, H., Saitoh, T., Sone, T., Guan, J. L., Akira, S., Imamoto, F., Noda, T., and Yoshimori, T. (2011) The LC3 recruitment mechanism is separate from Atg9L1-dependent membrane formation in the autophagic response against Salmonella. *Molecular biology of the cell* **22**, 2290-2300

55.   Starr, T., Child, R., Wehrly, T. D., Hansen, B., Hwang, S., Lopez-Otin, C., Virgin, H. W., and Celli, J. (2012) Selective subversion of autophagy complexes facilitates completion of the Brucella intracellular cycle. *Cell Host Microbe* **11**, 33-45

56.   Karanasios, E., Stapleton, E., Manifava, M., Kaizuka, T., Mizushima, N., Walker, S. A., and Ktistakis, N. T. (2013) Dynamic association of the ULK1 complex with omegasomes during autophagy induction. *J Cell Sci* **126**, 5224-5238

57.   Egan, D. F., Chun, M. G., Vamos, M., Zou, H., Rong, J., Miller, C. J., Lou, H. J., Raveendra-Panickar, D., Yang, C. C., Sheffler, D. J., Teriete, P., Asara, J. M., Turk, B. E., Cosford, N. D., and Shaw, R. J. (2015) Small Molecule Inhibition of the Autophagy Kinase ULK1 and Identification of ULK1 Substrates. *Mol Cell* **59**, 285-297

58.   Petherick, K. J., Conway, O. J., Mpamhanga, C., Osborne, S. A., Kamal, A., Saxty, B., and Ganley, I. G. (2015) Pharmacological inhibition of ULK1 kinase blocks mammalian target of rapamycin (mTOR)-dependent autophagy. *J Biol Chem* **290**, 28726

59.   Lazarus, M. B., and Shokat, K. M. (2015) Discovery and structure of a new inhibitor scaffold of the autophagy initiating kinase ULK1. *Bioorganic & medicinal chemistry* **23**, 5483-5488

60.   Maurer, K., Reyes-Robles, T., Alonzo, F., 3rd, Durbin, J., Torres, V. J., and Cadwell, K. (2015) Autophagy mediates tolerance to Staphylococcus aureus alpha-toxin. *Cell Host Microbe* **17**, 429-440

61.   O'Keeffe, K. M., Wilk, M. M., Leech, J. M., Murphy, A. G., Laabei, M., Monk, I. R., Massey, R. C., Lindsay, J. A., Foster, T. J., Geoghegan, J. A., and McLoughlin, R. M. (2015) Manipulation of Autophagy in Phagocytes Facilitates Staphylococcus aureus Bloodstream Infection. *Infect Immun* **83**, 3445-3457

62.   Chauhan, S., Kumar, S., Jain, A., Ponpuak, M., Mudd, M. H., Kimura, T., Choi, S. W., Peters, R., Mandell, M., Bruun, J. A., Johansen, T., and Deretic, V. (2016) TRIMs and Galectins Globally Cooperate and TRIM16 and Galectin-3 Co-direct Autophagy in Endomembrane Damage Homeostasis. *Dev Cell* **39**, 13-27

63.   Jia, J., Abudu, Y. P., Claude-Taupin, A., Gu, Y., Kumar, S., Choi, S. W., Peters, R., Mudd, M. H., Allers, L., Salemi, M., Phinney, B., Johansen, T., and Deretic, V. (2018) Galectins Control mTOR in Response to Endomembrane Damage. *Mol Cell* **70**, 120-135 e128

64.   Egan, D. F., Shackelford, D. B., Mihaylova, M. M., Gelino, S., Kohnz, R. A., Mair, W., Vasquez, D. S., Joshi, A., Gwinn, D. M., Taylor, R., Asara, J. M., Fitzpatrick, J., Dillin, A., Viollet, B., Kundu, M., Hansen, M., and Shaw, R. J. (2011) Phosphorylation of ULK1 (hATG1) by AMP-activated protein kinase connects energy sensing to mitophagy. *Science* **331**, 456-461

65. Dooley, H. C., Razi, M., Polson, H. E., Girardin, S. E., Wilson, M. I., and Tooze, S. A. (2014) WIPI2 links LC3 conjugation with PI3P, autophagosome formation, and pathogen clearance by recruiting Atg12-5-16L1. *Mol Cell* **55**, 238-252

66. Thurston, T. L., Boyle, K. B., Allen, M., Ravenhill, B. J., Karpiyevich, M., Bloor, S., Kaul, A., Noad, J., Foeglein, A., Matthews, S. A., Komander, D., Bycroft, M., and Randow, F. (2016) Recruitment of TBK1 to cytosol-invading Salmonella induces WIPI2-dependent antibacterial autophagy. *The EMBO journal* **35**, 1779-1792

67. Horn, J., Stelzner, K., Rudel, T., and Fraunholz, M. (2018) Inside job: Staphylococcus aureus host-pathogen interactions. *Int J Med Microbiol* **308**, 607-624

68. Vazquez, C. L., and Colombo, M. I. (2010) Coxiella burnetii modulates Beclin 1 and Bcl-2, preventing host cell apoptosis to generate a persistent bacterial infection. *Cell Death Differ* **17**, 421-438

69. Winchell, C. G., Graham, J. G., Kurten, R. C., and Voth, D. E. (2014) Coxiella burnetii type IV secretion-dependent recruitment of macrophage autophagosomes. *Infect Immun* **82**, 2229-2238

70. Beron, W., Gutierrez, M. G., Rabinovitch, M., and Colombo, M. I. (2002) Coxiella burnetii localizes in a Rab7-labeled compartment with autophagic characteristics. *Infect Immun* **70**, 5816-5821

71. Hosokawa, N., Hara, T., Kaizuka, T., Kishi, C., Takamura, A., Miura, Y., Iemura, S., Natsume, T., Takehana, K., Yamada, N., Guan, J. L., Oshiro, N., and Mizushima, N. (2009) Nutrient-dependent mTORC1 association with the ULK1-Atg13-FIP200 complex required for autophagy. *Molecular biology of the cell* **20**, 1981-1991

72. Itakura, E., and Mizushima, N. (2011) p62 Targeting to the autophagosome formation site requires self-oligomerization but not LC3 binding. *J Cell Biol* **192**, 17-27

73. Sanjana, N. E., Shalem, O., and Zhang, F. (2014) Improved vectors and genome-wide libraries for CRISPR screening. *Nat Methods* **11**, 783-784

74. Joung, J., Konermann, S., Gootenberg, J. S., Abudayyeh, O. O., Platt, R. J., Brigham, M. D., Sanjana, N. E., and Zhang, F. (2017) Genome-scale CRISPR-Cas9 knockout and transcriptional activation screening. *Nat Protoc* **12**, 828-863

75. Maycotte, P., Aryal, S., Cummings, C. T., Thorburn, J., Morgan, M. J., and Thorburn, A. (2012) Chloroquine sensitizes breast cancer cells to chemotherapy independent of autophagy. *Autophagy* **8**, 200-212
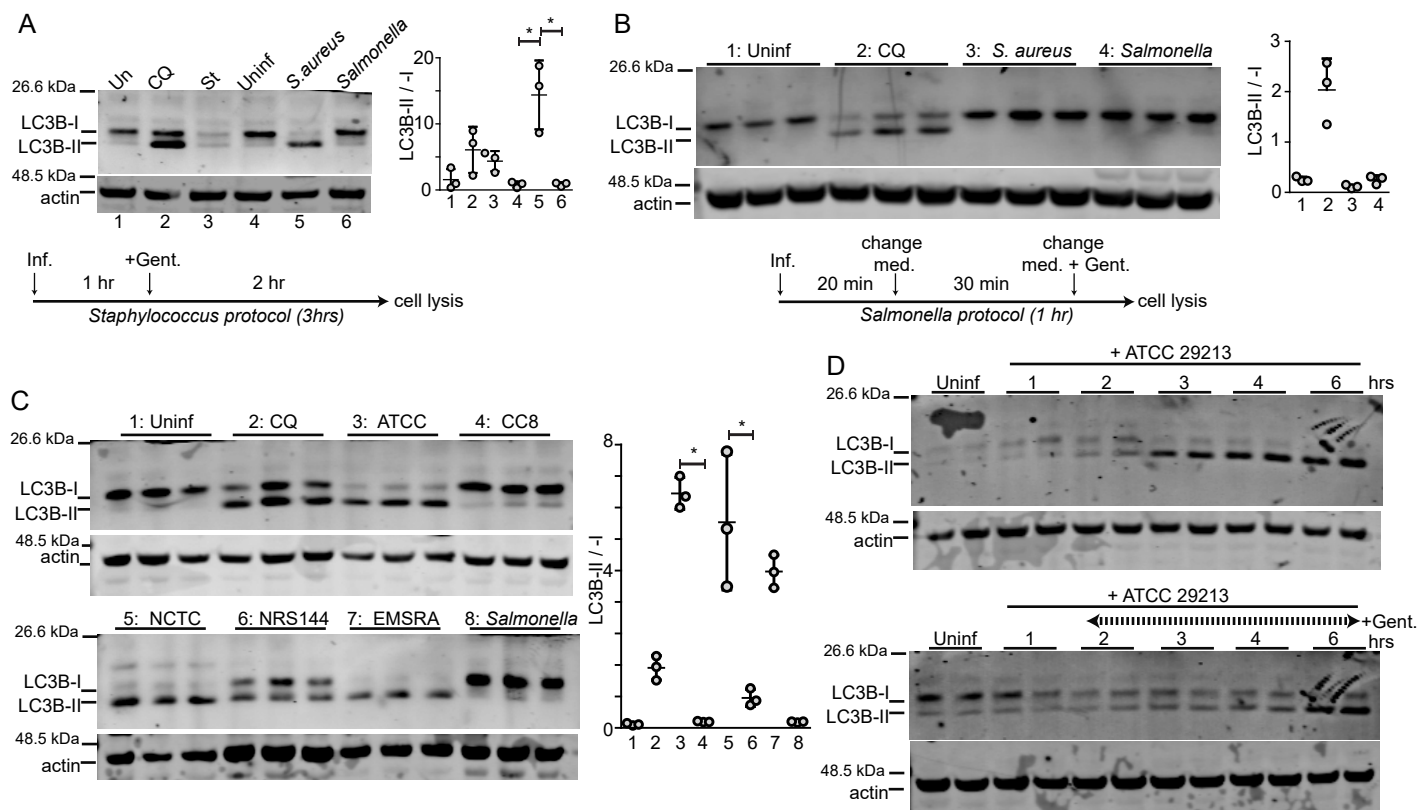
Figure 1. Activation of autophagy in HeLa cells following invasion of *Staphylococcus aureus* and *Salmonella enterica sv. Typhimurium*. HeLa cells were infected with *Staphylococcus aureus* (ATCC29213) or *Salmonella enterica sv. Typhimurium* (NCTC13347) using 2 different protocols (see Materials and Methods).

(A) Using the Staphylococcus protocol, bacteria were grown until OD=0.3 and used to infect cells at 200 MOI. One hour post infection, gentamicin (0.05 mg/ml) was added to inactivate extracellular bacteria and the infection proceeded for a further 2 hrs. As control, cells were treated with EBSS (AA and serum starvation) or chloroquine 25 µM and incubated for 3 hrs. Cell lysates were resolved by gel electrophoresis and proteins were probed with anti-LC3B antibody. Activation of autophagy was measured via ratio of LC3B-II / LC3B-I. Average from N=3 experiments ± SD shown. (*) P < 0.001 by ANOVA and Tukey's post test.

(B) Using the Salmonella protocol, bacteria were grown until OD=1.2-1.5 and then diluted 1:100. This diluted culture was used to infect cells for 20 min. and then changed to fresh cell media containing gentamycin. Infected (or control autophagy-stimulated) cells were lysed after 1 hr and analysed for LC3B lipidation. The average from N=3 samples ± SD is shown. (A and B) repeated three times on different days.

(C) HeLa cells were infected with *Staphylococcus aureus* strains (ATCC29213, clonal complex 8 isolate (CC8), NCTC8325, NRS144 agr-mutant or EMRSA LF78) or *Salmonella enterica sv Typhimurium* (N=3). Cells were infected at 200 MOI. One hour post infection, genatmycin was added and cells were further incubated for 3 hrs. Average from 3 samples ± SD shown. Representative of two experiments. (*) P < 0.001 by ANOVA and Tukey's post test.

(D) HeLa cells were infected with ATCC29213 at 100 MOI. Top: Cells were further incubated for up to 6 hrs. Bottom: Gentamicin (0.05 mg/ml) was added 1 hr after infection. N=2 replicates per condition.
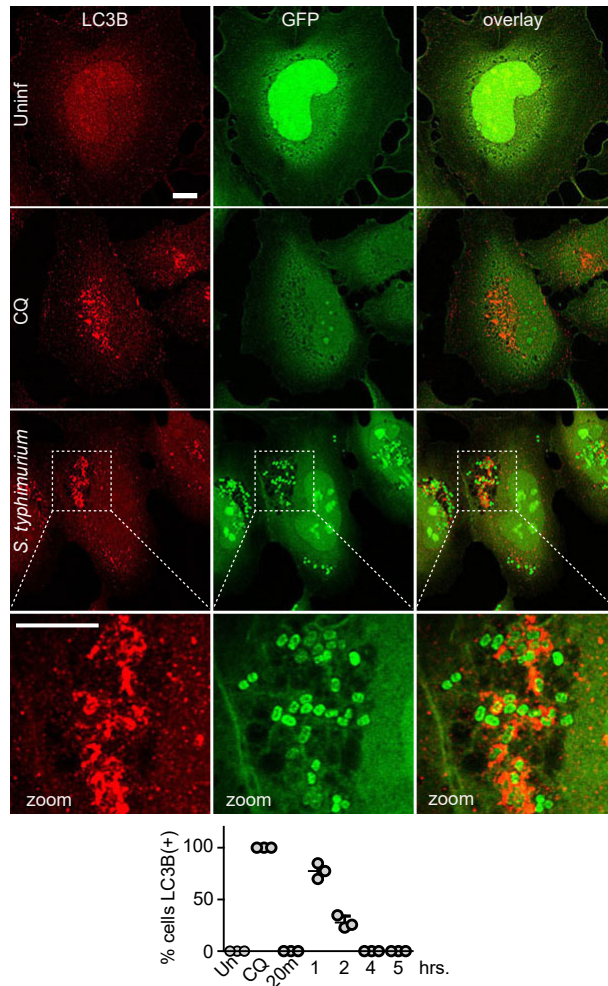
Figure 2. Autophagosome formation following infection by *Salmonella enterica sv. Typhimurium*.
HeLa cells were plated on glass coverslips. As control, cells were treated with chloroquine (CQ, 25 µM) for 3 hrs to cause autophagosome accumulation. Alternatively, cells were infected with 1:100 MOI of GFP expressing *Salmonella enterica sv. Typhimurium* for 1 hr using the Salmonella protocol. After treatments, cells were fixed and stained for LC3B(+) membranes. All scale bars: 10 µm. Zoom: 3.4x magnification. Bottom: HeLa cells were infected as above with 1:100 MOI GFP-Salmonella and incubated for 20 min, 1, 2, 3, or 5 hrs. Note: except for the 20 min timepoint, gentamycin was added 50 min after infection. The percentage of cells positive for LC3B puncta was counted (50-100 cells counted per sample). Average from N=3 samples ± SD.
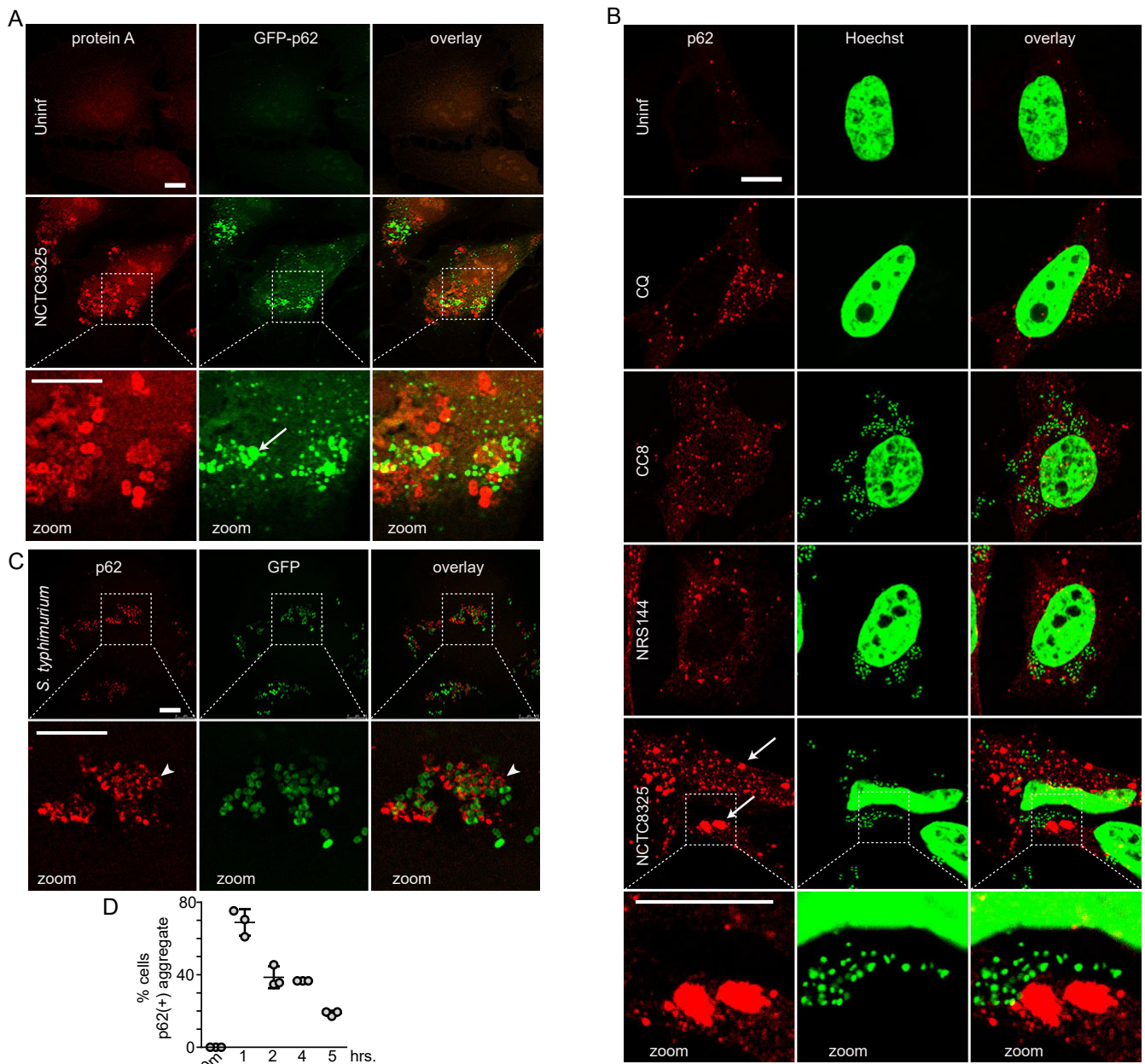
Figure 3. Differential formation of p62/Sequestosome1-positive membranes following infection by *Staphylococcus vs. Salmonella*.

(A) HeLa/GFP-p62 cells were infected with 100 MOI NCTC8325 for 3 hrs (gentamicin added after 1st hour). After fixation, bacteria were detected by anti-protein A staining. Arrow: p62(+) aggregate. All scale bars: 10 μm. All zoom: 3.4x magnification.

(B) HeLa cells were treated with chloroquine as control (CQ, 25 μM) or infected as above with indicated strains of *Staphylococcus aureus*. After fixation, cells were stained with antibodies for p62/SQSTM1 and Hoescht 33342 (detects bacterial and host cell DNA). Arrows: large size p62(+) aggregates.

(C) HeLa cells were infected with 1:100 diluted GFP-*Salmonella enterica sv. Typhimurium* for 1 hr before fixation and staining with antibodies for p62/SQSTM1. Arrowhead: co-localization of p62 on *Salmonella*.

(D) HeLa cells were infected with GFP-*Salmonella* as in (C) for the indicated times before fixation. The percentage of cells positive for p62(+) membranes was counted (40-110 cells counted per sample). Average from N=3 samples ± SD.
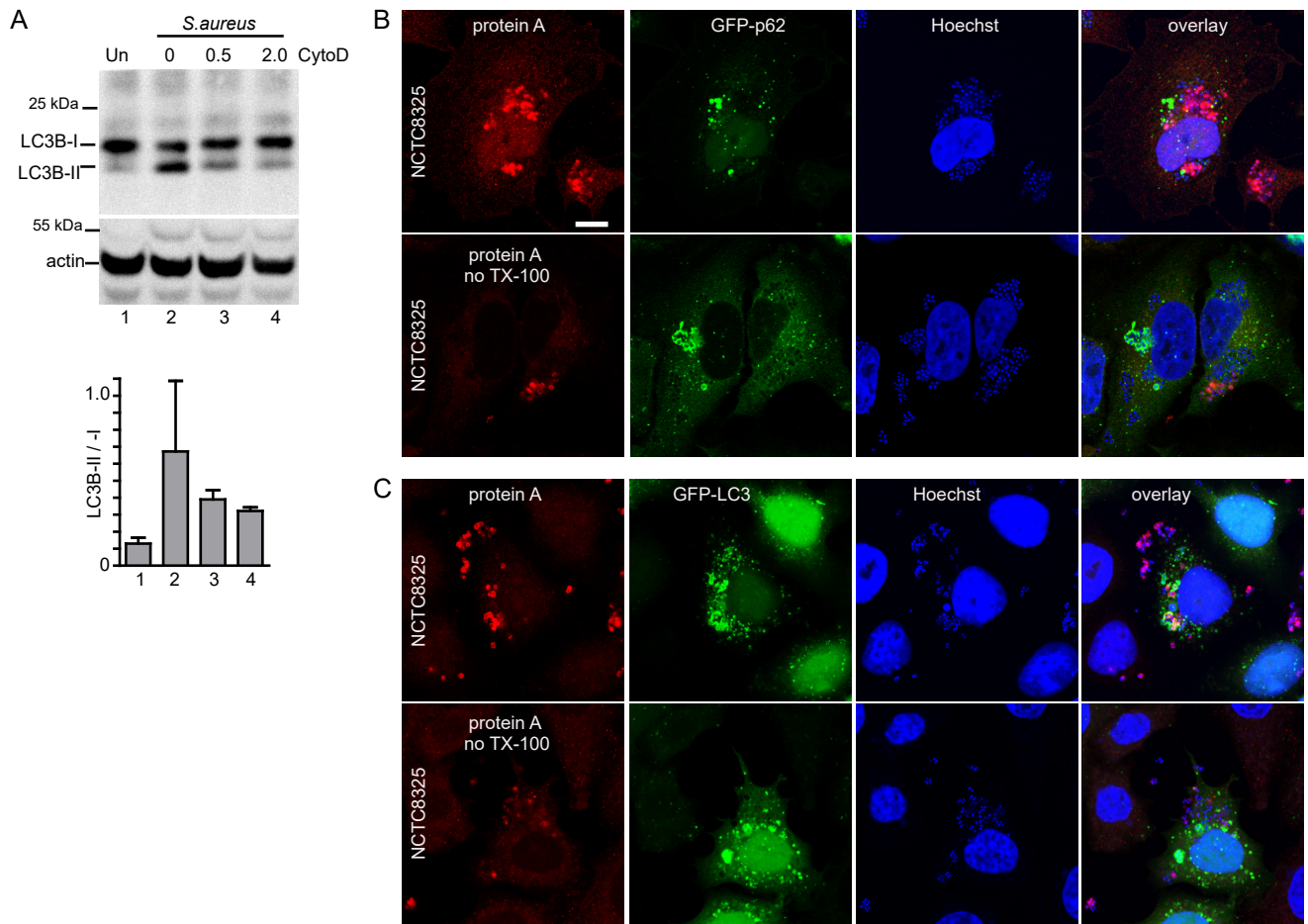
Figure 4. Intracellular *Staphylococcus* stimulate autophagosome formation
(A) HeLa cells were infected with 200 MOI NCTC8325 for 3 hrs. Where indicated, cell infections included cytochalasin D (µM). Activation of autophagy was measured via LC3B-II / LC3B-I. Average from N=3 experiments ± SD.
(B) HeLa/GFP-p62 cells were infected with 100 MOI NCTC8325 for 3 hrs (gentamicin added after first 1 hr of infection). After fixation, cells were stained for protein A and Hoescht 33342. Where indicated, cells were stained without permeablization by TX-100. Scale bar: 10 µm.
(C) HeLa/GFP-LC3 cells were infected and stained as in (B).
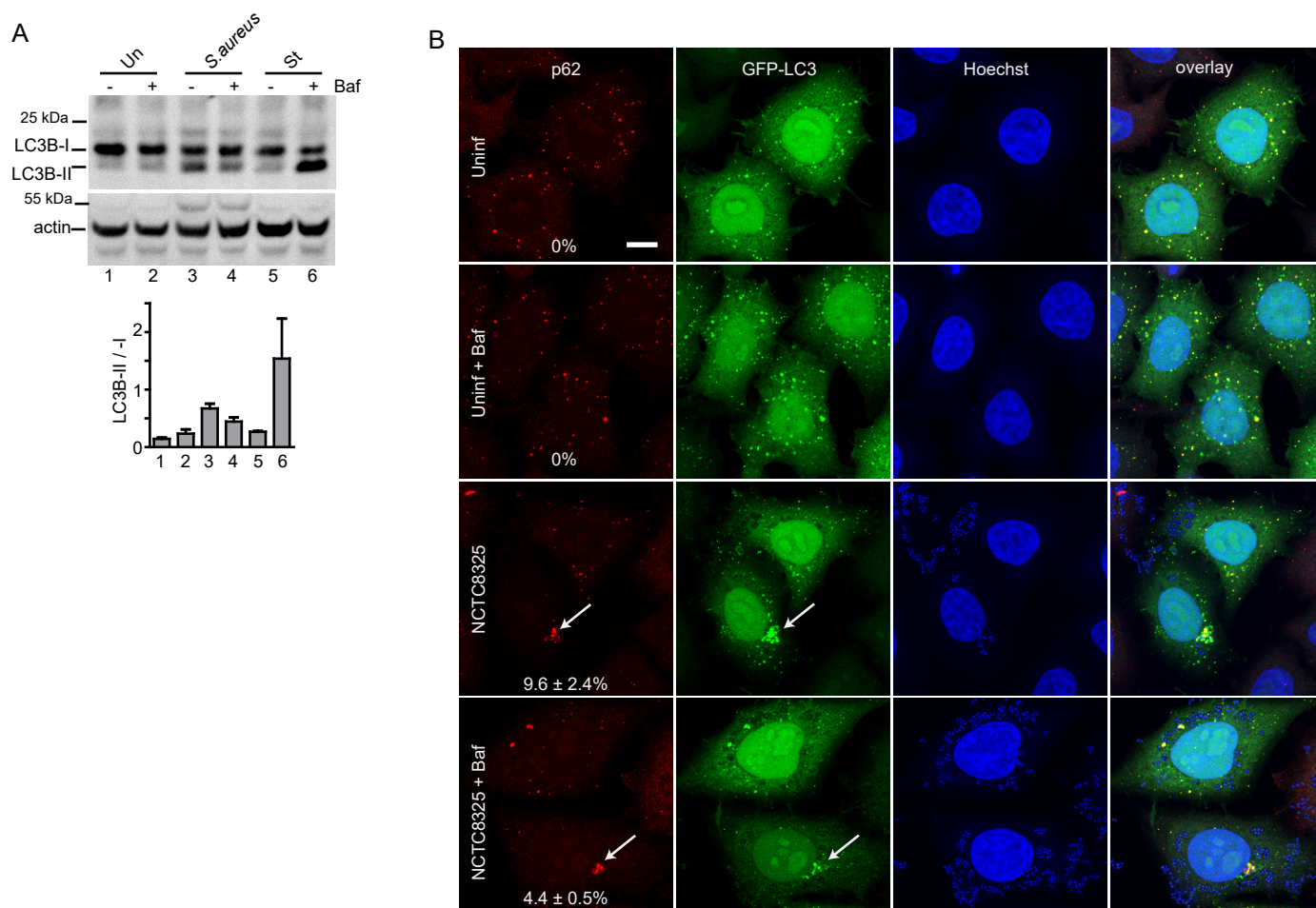
Figure 5. Autophagosomes generated following *Staphylococcus* infection do not show rapid flux.
(A) HeLa cells were infected with 200 MOI NCTC8325 or alternatively starved (St) in EBSS for 3 hrs. Where indicated, cell treatments included bafilomycin A1 (10 nM). Cell lysates were resolved by gel electrophoresis and probed with anti-LC3B antibody. Activation of autophagy was measured via LC3B-II / LC3B-I. Average from N=3 experiments ± SD.
(B) HeLa/GFP-LC3 cells were infected with 100 MOI NCTC8325 for 3 hrs (gentamicin added after first 1 hr of infection). Where indicated, cell treatments included bafilomycin A1. After fixation, cells were stained with antibodies for p62/SQSTM1 and Hoescht 33342. Scale bar: 10 μm. Arrows: large size p62(+) / GFP-LC3(+) aggregates. Shown are percentage cells (+) for large-size autophagosomes (N=3 samples ± SD; 100-250 cells counted per sample).
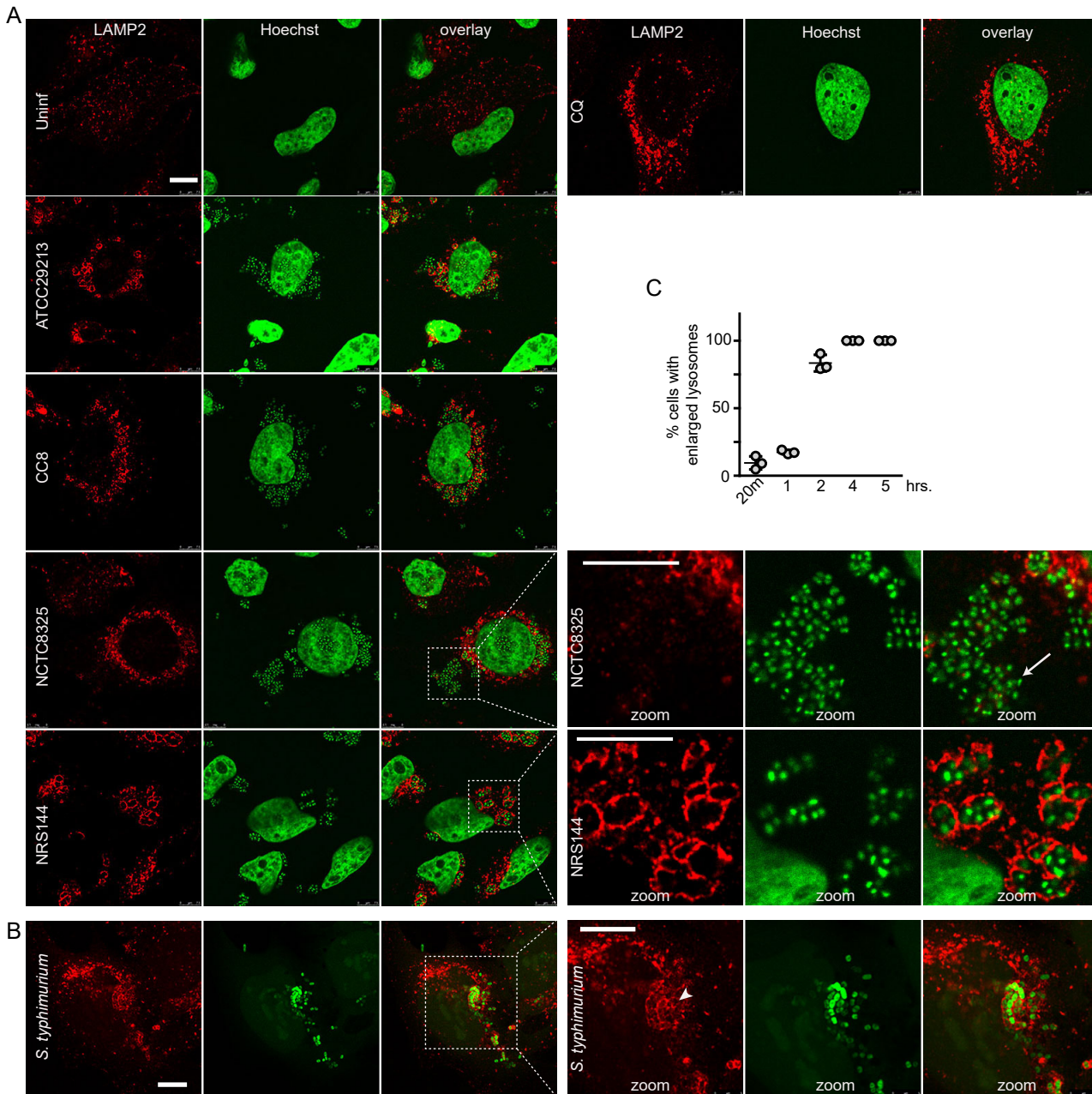
Figure 6. Escape of virulent strains of *Staphylococcus aureus* from swollen lysosomes.
(A) HeLa cells were treated with chloroquine as control for 3 hrs (CQ, 25 µM) or infected as in Fig 3B with different strains of *Staphylococcus aureus* (100 MOI, 3 hrs).   After fixation, cells were stained with antibodies for LAMP-2 and Hoescht 33342 (detects bacterial and host cell DNA). All scale bars: 10 µm.   Arrow, zoomed inset: *Staphylococcus aureus* after escape from LAMP-2(+) lysosomes. Zoom: 3.4x magnification.
(B) HeLa cells were infected with 1:100 diluted GFP-*Salmonella enterica sv. Typhimurium*.   After 5 hrs, cells were fixed and stained for LAMP-2. Arrowhead, zoomed inset: *Salmonella* still confined within LAMP-2(+) lysosomes. Zoom: 1.9x magnification.
(C) HeLa cells infected with GFP-*Salmonella* as in (B) for different times were quantified for percentage of cells containing swollen LAMP-2(+) lysosomes (40-85 cells counted per sample). Average from N=3 samples ± SD.
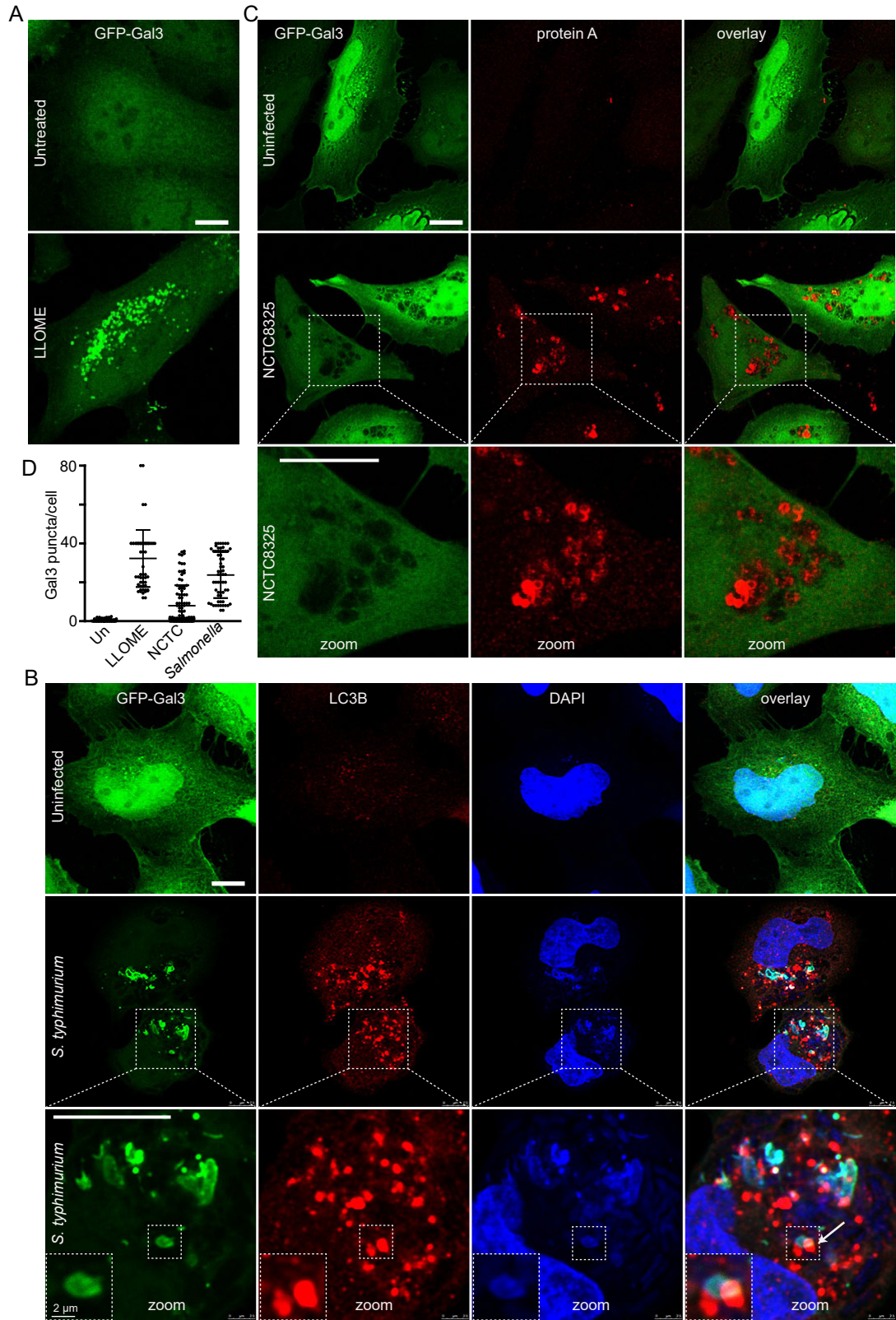
Figure 7. *Staphylococcus aureus* **infection does not generate lysosome damage signals.**

(A,C) HeLa cells were transfected to express GFP-Galectin3 (GFP-Gal3). As control, cells were treated with LLOME (2mM for 3 hrs) to induce lysosomal damage and Gal3(+) puncta. (C) Alternatively, cells were infected with *Staphylococcus aureus* NCTC8325 (100 MOI, 5 hrs). All (non-labelled) scale bars: 10 μm. Zoom: 3.0x magnification.

(B) HeLa cells transfected with GFP-Gal3 were infected with 1:100 diluted *Salmonella enterica sv. Typhimurium* for 3 hrs (gentamicin added after first 50 min of infection). Cells were fixed and co-stained with LC3B antibody (to detect autophagosomes) and DAPI (to detect *Salmonella*). Arrow, zoomed insets: LC3B recruitment to sites of *Salmonella*-induced lysosomal damage marked by Gal3. Zoom: 3.6x magnification (with further 2.0x magnification, inset).

(D) HeLa cells transfected with GFP-Gal3 were infected with 1:100 diluted *Salmonella enterica Sv. Typhimurium* (using Salmonella protocol) or 100 MOI of NCTC8325 (using Staphylococcus protocol) for 5 hrs (for comparison, positive control cells were treated with LLOME for 3 hrs). Gal3 puncta were quantified. Average puncta/cell from N=50-100 cells from 2 independent experiments ± SD.
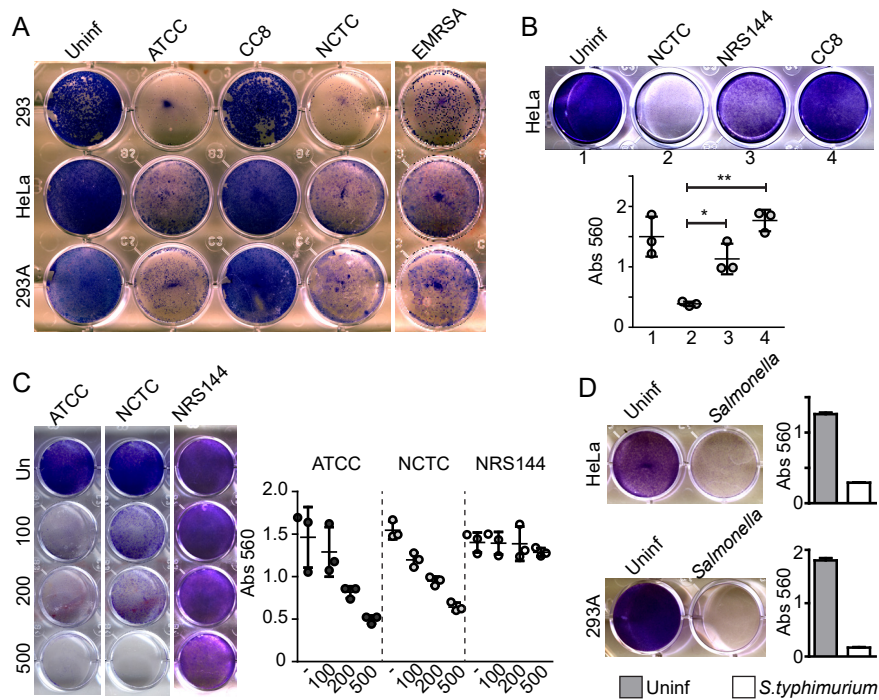
Figure 8. Death of host cells upon infection by *Staphylococcus* and *Salmonella*.

(A) Indicated host cell lines were infected with 100 MOI of varying *Staphylococcus strains* (ATCC29263, CC8, NCTC8325, or EMRSA LF78). After 1 hr of infection, gentamicin was added to the media and cells were further incubated for 72 hrs before fixation and Giemsa staining of remaining viable cells.

(B) HeLa cells were infected as indicated with 200 MOI *Staphylococcus aureus* for 72 hrs (gentamycin added after 1st hour of infection). Viable cells staining with Giemsa were quantified via absorbance. Average from N=3 ± SD. Representative of 2 experiments. (**) P < 0.001, (*) P < 0.01 by ANOVA and Tukey's post test.

(C) HeLa cells were infected as indicated with varying MOI and quantified as in (B). Average from N=3 ± SD.

(D) HeLa or HEK293A cells were infected with 1:100 diluted *Salmonella enterica Sv. Typhimurium* (using Salmonella protocol) and incubated for 72 hrs before fixation, staining and quantification. Average from N=2 ± range.
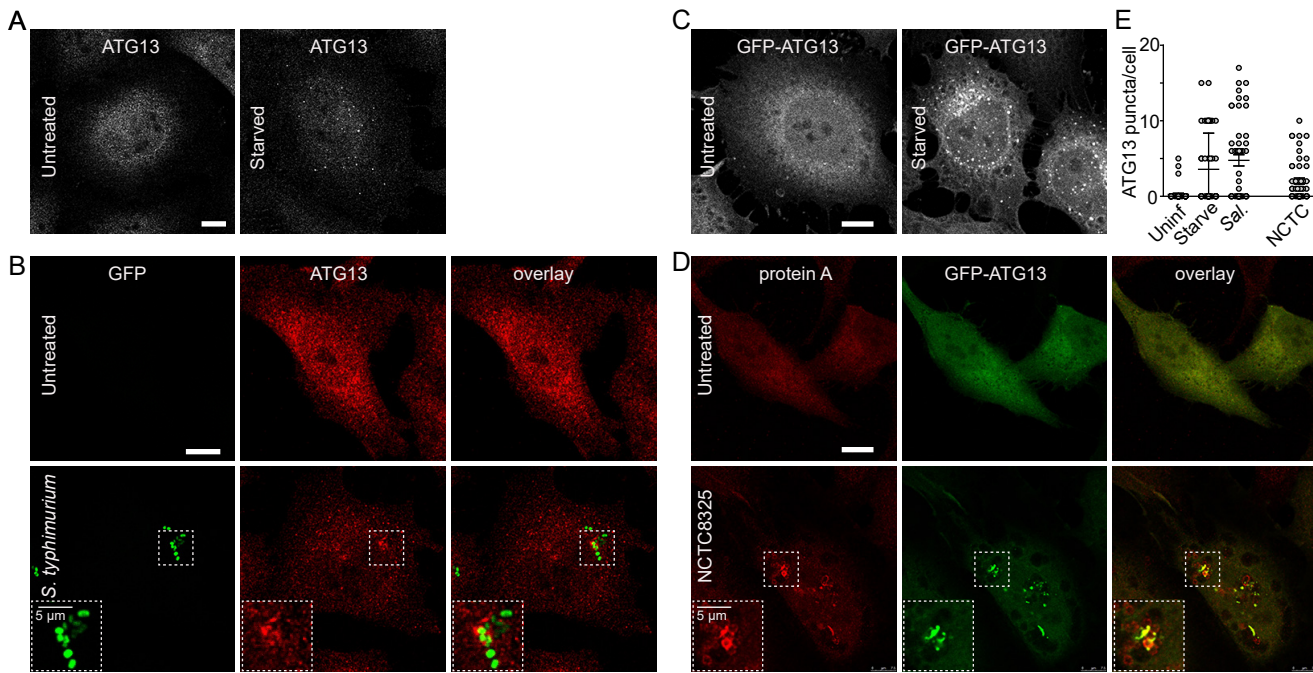
Figure 9. *Staphylococcus* **and** *Salmonella* **infection both promote recruitment of ATG13 to bacteria-associated autophagosome membranes.**

(A) As control, HeLa cells were left untreated or starved in EBSS for 1 hr before fixation and antibody staining to detect endogenous ATG13. Scale bars: 10 μm.

(B) HeLa cells were infected with 1:100 diluted *Salmonella enterica Sv. Typhimurium* for 1 hr and stained as in (A).

(C) HeLa/GFP-ATG13 cells were starved as in (A).

(D) HeLa/GFP-ATG13 cells were infected with *Staphylococcus aureus* NCTC8325 for 3 hrs, fixed and stained with anti-protein A antibody. Zoomed insets (2.0x magnification) highlight ATG13 localizing to invading *Salmonella* or *Staphylococcus*.

(E) HeLa/GFP-ATG13 cells were untreated, starved in EBSS or infected with *Salmonella enterica Sv. Typhimurium* for 1 hr. For comparison, cells were infected with NCTC8325 for 3 hrs. After fixation, cells were stained with DAPI and GFP-ATG13(+) puncta were quantified. Average puncta/cell from N=50 cells ± SD (representative of 2 independent experiments).
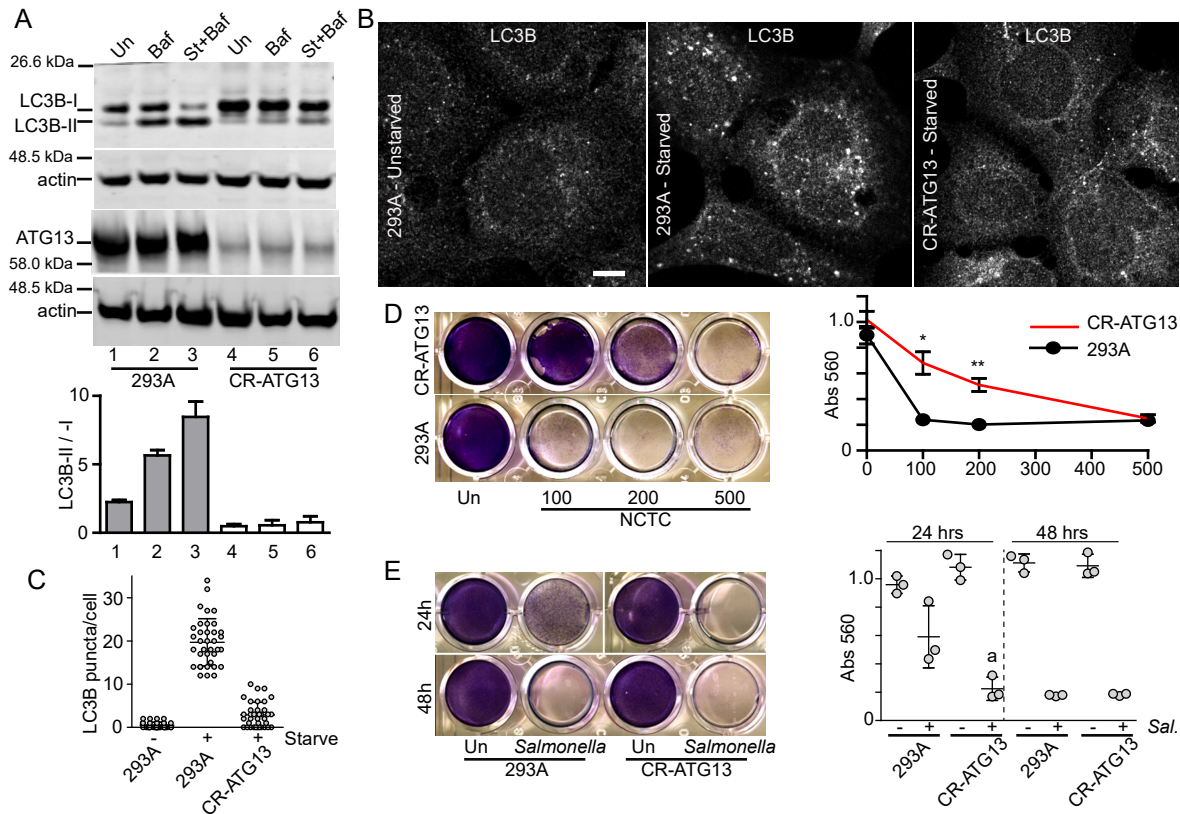
Figure 10. Inhibition of ATG13-dependent autophagy suppresses *Staphylococcus*-induced cell death.
(A) ATG13 was targeted in HEK293A cells using the CRISPR-Cas9 system (CR-ATG13). Wildtype HEK293A or CR-ATG13 cells were treated to bafilomycin A1 (10 nM) +/- starvation in EBSS for 2 hrs. Cell lysates were analysed for LC3B lipidation as in Fig 1. N=2 ± range.
(B,C) Wildtype HEK293A or CR-ATG13 cells were starved in EBSS for 2 hrs, fixed and stained to detect LC3B puncta. Average puncta/cell from N=36 cells ± SD. Scale bar: 10 μm
(D) Wildtype HEK293A or CR-ATG13 cells were infected with varying MOI of *Staphylococcus aureus* NCTC8325 and assayed for cell viability as in Fig 6. (**) P<0.001; (*) P<0.01 by un-paired t-test: CR-ATG13 vs. 293A (comparing equivalent MOI).
(E) Wildtype HEK293A or CR-ATG13 cells were infected with 1:100 diluted *Salmonella enterica Sv. Typhimurium* and incubated for 24 or 48 hrs before staining for cell viability. Averages from N=3 ± SD. (a) P= 0.054 by t-test: infected CR-ATG13 vs 293A at 24 hr.
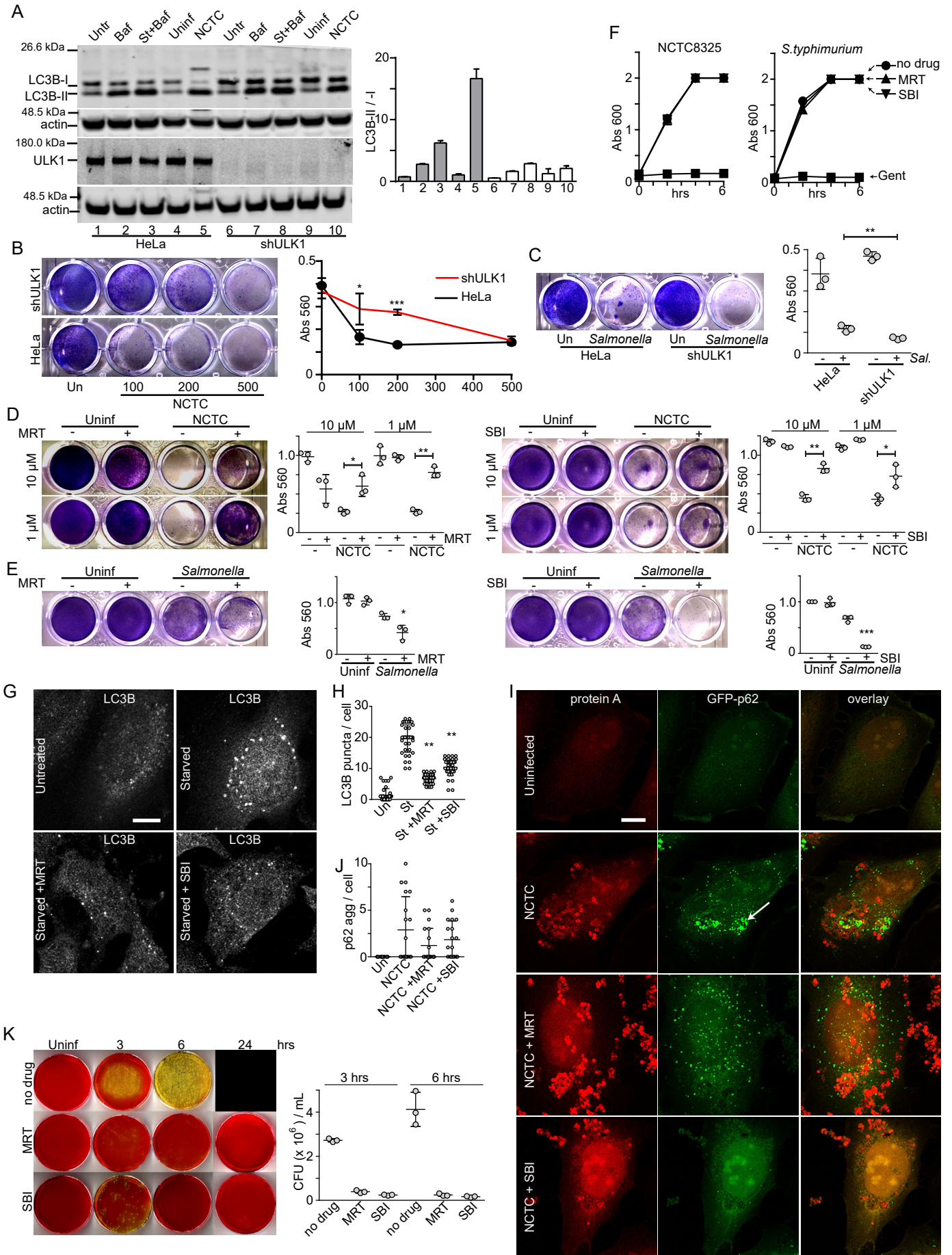
Figure 11. Inhibition of ULK1 suppresses *Staphylococcus* intracellular replication and host cell death.

(A) ULK1 was targeted in HeLa cells using shRNA (shULK1). Wildtype HeLa or shULK1 cells were treated to bafilomycin A1 (10 nM) +/- starvation in EBSS for 2 hrs. Cell lysates were analysed and quantified for LC3B lipidation as in Fig 1. N=2 ± range.

(B) Wildtype HeLa or shULK1 cells were infected with varying MOI of *Staphylococcus aureus* NCTC8325 and assayed for cell viability as in Fig 6. Averages of N=3 ± SD. (***) P<0.001; (*) P<0.05 by un-paired t-test: shULK1 vs. HeLa (comparing equivalent MOI).

(C) Wildtype HeLa or shULK1 cells were infected with 1:100 diluted *Salmonella enterica Sv. Typhimurium* and incubated for 72 hrs before staining for cell viability. Averages of N=3 ± SD. (**) P<0.01 by un-paired t-test.

(D) HEK293A cells were infected with NCTC8325 (200 MOI). At the time of infection, ULK1 inhibitors MRT68921 or SBI-0206965 were added at 1 or 10 μM. Gentamicin (0.05 mg/ml) was added 1 hr post infection. Cells were incubated for 48 hrs and assayed for cell viability as in Fig 6. Averages of N=3 ± SD.

(E) HEK293A cells were infected with 1:100 diluted *Salmonella* as in (C). At the time of infection, ULK1 inhibitors were added at 10 μM. Gentamicin was added 50 min post infection. Cells were incubated for 24 hrs and assayed for cell viability. Shown are averages from N=3 ± SD. (D,E) (***) P<0.0001; (**) P<0.001; (*) P<0.05 by un-paired t-test: infected cells comparing (+) vs (-) ULK1 inhibitor.

(F) *Staphylococcus* NCTC8325 or *Salmonella enterica sv. Typhimurium* cultures were diluted 1:100 and grown in the presence of ULK1 inhibitors (10 μM) or gentamicin (0.05 mg/ml). Averages of N=3 ± SD.

(G,H) HeLa cells were incubated in EBSS for 2 hrs in the presence or absence of ULK1 inhibitors (10 μM). After fixation, cells were stained with anti-LC3B antibody. Scale bars: 10 µm. Average LC3B(+) puncta /cell from N=40 cells per condition ± SD. (**) P<0.001 vs starved no-drug control by ANOVA and Tukey's post test.

(I,J) HeLa/GFP-p62 stable cells were infected with NCTC8325 (100 MOI) for 3 hrs in the presence or absence of ULK1 inhibitors (10 µM). After fixation, cells were stained with anti-protein A antibody. Scale bars: 10 µm. Arrow: Large-sized p62 aggregates induced by NCTC8325 infection. Average large GFP-p62 aggregates /cell from N=20 cells per condition ± SD. Representative of two experiments.

(K) HEK293A cells were infected with NCTC8325 (100 MOI) in the presence of MRT68921 (1 µM) or SBI-0206965 (10 µM). Gentamicin (0.05 mg/ml) was added 1 hr post infection. Cells were further incubated 3, 6 or 24 hrs before lysis. Bacterial titres in cell lysates were measured by growth on solid media. Average CFU/ml from 3 and 6 hrs timepoints (N=3 ± SD) shown. Bacterial growth changes colour of phenol red in bacterial plates. No host cells remained 24 hrs after infection in the absence of ULK1 inhibitor.

Inhibition of the ULK1 protein complex suppresses *Staphylococcus*-induced autophagy and cell death

Ohood A. Radhi, Scott Davidson, Fiona Scott, Run X. Zeng, D. Heulyn Jones, Nicholas C.O. Tomkinson, Jun Yu and Edmond Y.W. Chan

Access the most updated version of this article at doi: 10.1074/jbc.RA119.008923

Alerts:
- When this article is cited
- When a correction for this article is posted

Click here to choose from all of JBC's e-mail alerts